

Research Article

The characteristics and preservation potential of Hurricane Irma's overwash deposit in southern Florida, USA

Kristen M. Joyse^{a,b,*}, Nicole S. Khan^c, Ryan P. Moyer^{d,e}, Kara R. Radabaugh^d, Isabel Hong^{f,g}, Amanda R. Chappel^{d,h}, Jennifer S. Walker^a, Christian J. Sandersⁱ, Simon E. Engelhart^j, Robert E. Kopp^{a,k}, Benjamin P. Horton^{b,l}

^a Department of Earth and Planetary Sciences, Rutgers University, Piscataway, NJ, USA

^b Earth Observatory of Singapore, Nanyang Technological University, Singapore

^c Department of Earth Sciences, The University of Hong Kong, Hong Kong

^d Florida Fish and Wildlife Conservation Commission, Fish and Wildlife Research Institute, Saint Petersburg, FL, USA

^e TerraCarbon, LLC, Saint Petersburg, FL, USA

^f Department of Geography and the Environment, Villanova University, Villanova, PA, USA

^g Department of Geological Sciences, Central Washington University, Ellensburg, WA, USA

^h Department of Environmental Engineering Sciences, University of Florida, Gainesville, FL, USA

ⁱ National Marine Science Centre, Southern Cross University, Coffs Harbour, New South Wales, Australia

^j Department of Geography, Durham University, Durham, UK

^k Institute of Earth, Ocean, and Atmospheric Sciences, Rutgers University, New Brunswick, NJ, USA

^l Asian School of the Environment, Nanyang Technological University, Singapore

ARTICLE INFO

Editor: Edward Anthony

Keywords:

Overwash deposit
Mangrove
Storm surge
Hurricane
Carbonate
Paleotempestology

ABSTRACT

Overwash deposits from tropical cyclone-induced storm surges are commonly used as modern analogues for paleo-storm studies. However, the evolution of these deposits between their time of deposition and their incorporation into the geologic record is poorly understood. To understand how the characteristics of an overwash deposit can change over time, we analyzed overwash deposits from four mangrove islands in southern Florida two to three months and twenty-two months after Hurricane Irma's landfall in the region on 10 September 2017. We analyzed the stratigraphy, mean grain size, organic and carbonate contents, stable carbon isotopic signatures, and microfossil (foraminifera and diatom) assemblages of pre-Irma and Irma overwash sediments. Hurricane Irma's storm surge deposited light gray carbonate muds and sands up to 11 cm thick over red organic-rich mangrove peats throughout mangrove islands in southern Florida. Stratigraphy, grain size, loss-on-ignition, and foraminifera analyses provided the strongest evidence for differentiating Irma's overwash deposit from underlying mangrove peats and, if preserved, are expected to identify Hurricane Irma's overwash event within the geologic record. Mean grain size showed the overwash deposit ($5.0 \pm 0.8 \phi$) was coarser than underlying mangrove peats ($6.7 \pm 0.7 \phi$), and loss-on-ignition showed the overwash deposit had a lower organic content ($19.8 \pm 9.1\%$) and a higher carbonate content ($67.8 \pm 20.7\%$) than the underlying peats ($59.4 \pm 14.6\%$ and $33.7 \pm 11.0\%$, respectively). The overwash deposit was dominated by a diverse, abundant assemblage of sub-tidal benthic calcareous foraminifera compared to a uniform, sparse assemblage of agglutinated foraminifera in the pre-Irma mangrove peats. Geochemical indicators were not able to provide evidence of an overwash event by differentiating organic $\delta^{13}\text{C}$ or C/N of the overwash deposit from those of the mangrove peats. The complex relationship between diatoms and local environmental factors prevented diatom assemblages from providing a statistically clear distinction between Irma's overwash sediments and underlying mangrove peats. By visiting Hurricane Irma's overwash deposit immediately following landfall and nearly two years post-storm, we were able to document how the overwash deposit's characteristics changed over time. Continued monitoring on the scale of five to ten years would provide further insights into the preservation of overwash deposits for paleo-storm studies.

* Corresponding author at: Earth Observatory of Singapore, Nanyang Technological University, Singapore.

E-mail address: kristenmarie.joyse@ntu.edu.sg (K.M. Joyse).

<https://doi.org/10.1016/j.margeo.2023.107077>

Received 8 October 2022; Received in revised form 16 May 2023; Accepted 23 May 2023

Available online 26 May 2023

0025-3227/© 2023 The Authors. Published by Elsevier B.V. This is an open access article under the CC BY-NC-ND license (<http://creativecommons.org/licenses/by-nc-nd/4.0/>).

1. Introduction

Extreme flooding from storm surges causes substantial damages to coastal communities in terms of damages to infrastructure and loss of life (Lin et al., 2012). Storm surges are rises in water level above predicted tides, which can be generated by storms, such as tropical cyclones (Brandon et al., 2014). The storm surges can transport sediments from nearshore and beach environments (Schwartz, 1975; Liu, 2004) landward to low-energy coastal environments in fan-shaped overwash deposits (Fig. 1) (e.g., Liu and Fearn, 2000; Liu, 2004; Donnelly and Webb

III, 2004). Distinguishing the properties of an overwash deposit from those of the low-energy coastal sediments is fundamental to identifying storm-surge events in the geologic record (e.g., Liu and Fearn, 2000; Donnelly et al., 2001a; Scileppi and Donnelly, 2007). Reliable geologic records of tropical cyclone activity prior to instrumental tide gauge records are important to provide empirical constraints on tropical cyclone trends and risks and to better understand the influence of climate change on landfalling tropical cyclones (e.g., Reed et al., 2015; Lin et al., 2016; Garner et al., 2017). Empirical constraints are important because model predictions indicate the proportion of extreme tropical cyclones to

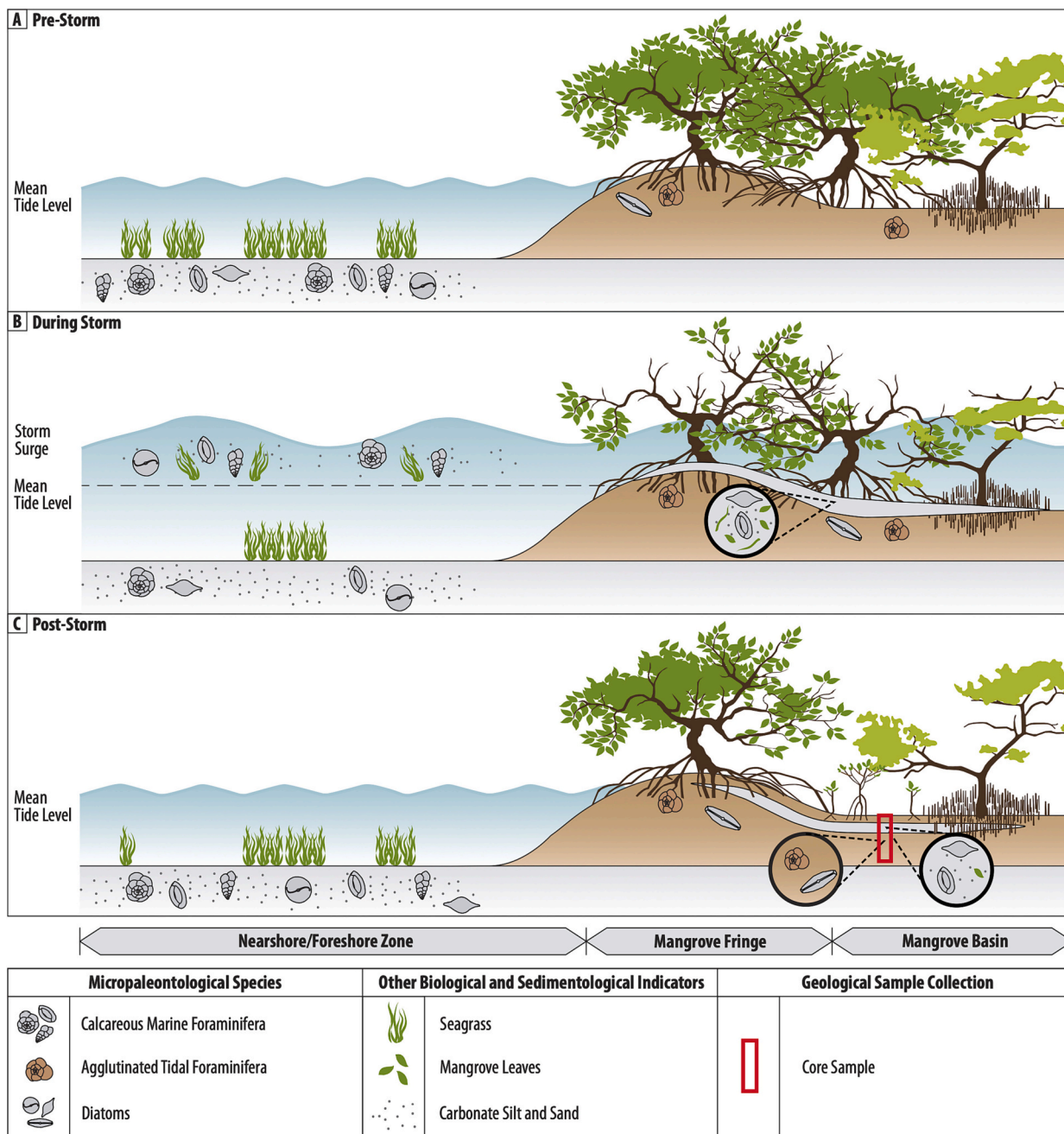


Fig. 1. Idealized cross-section of tropical mangrove environment with sedimentary and micropaleontological indicators used to contrast marine originating overwash deposits and brackish mangrove peat sediments. (A) Pre-storm; Left: Shallow marine environment with sea grass, diverse calcareous foraminifera species, marine and brackish diatom species, coarse-grained carbonate sediments, and mean tidal level. Right: Mangrove forest with fringe adjacent to shoreline and basin landwards. Organic-rich red mangrove peat with few agglutinated foraminifera and freshwater diatoms residing on forest floor. (B) During storm; Storm surge suspends and transports coarser-grained carbonate sediments and biologic components from offshore into mangrove forest. An overwash deposit is deposited within the mangrove forest. (C) Post-storm; Deposition of organic mud and peat formation resumes preserving the overwash deposit into the geologic record. (For interpretation of the references to colour in this figure legend, the reader is referred to the web version of this article.)

increase over time, while the overall number of tropical cyclones is expected to remain similar (Arias et al., 2021).

Geologic records of overwash deposits from tropical cyclones are stratigraphically visible in sediment cores, tidal channel bank exposures, and outcrops in low-energy coastal environments such as salt marshes, mangroves, and lagoons (e.g., Kiage et al., 2011; McCloskey and Liu, 2012; Bregy et al., 2018). Overwash deposits are often identifiable within coastal stratigraphy by a sharp, erosional contact at their base and a gradational contact above (e.g., Liu and Fearn, 2000; Donnelly et al., 2004; Denommee et al., 2014) and by a larger grain size and a lower organic content than the surrounding sediments (e.g., Donnelly et al., 2001a, 2001b, 2004). Microfossils (e.g., foraminifera and diatoms) (e.g., Hippensteel et al., 1999; Hippensteel and Garcia, 2014; Kosciuch et al., 2018) and biogeochemical indicators (e.g., $\delta^{13}\text{C}$ and C/

N) (e.g., Lambert et al., 2008; Das et al., 2013; Breithaupt et al., 2019) have been used to further identify geologic records of overwash deposits. The ecological zonation of modern foraminifera and diatom species within a coastal environment can be used to classify the transport and deposition of allochthonous sediments via storm surge (e.g., Hippensteel et al., 1999; Pilarczyk et al., 2014; Kosciuch et al., 2018; Wang et al., 2019). Similarly, stable carbon isotope geochemistry in conjunction with organic carbon and total nitrogen content ratios (C/N) of coastal sediments can be indicative of terrestrial and brackish versus marine sediment origins (Khan et al., 2015a), making geochemical signatures useful in identifying overwash deposits based on sediment source (e.g., Lamb et al., 2006; Kemp et al., 2010; Khan et al., 2015b).

Reconstructing geologic records of overwash deposits relies on modern analogue studies to describe their endmember characteristics,

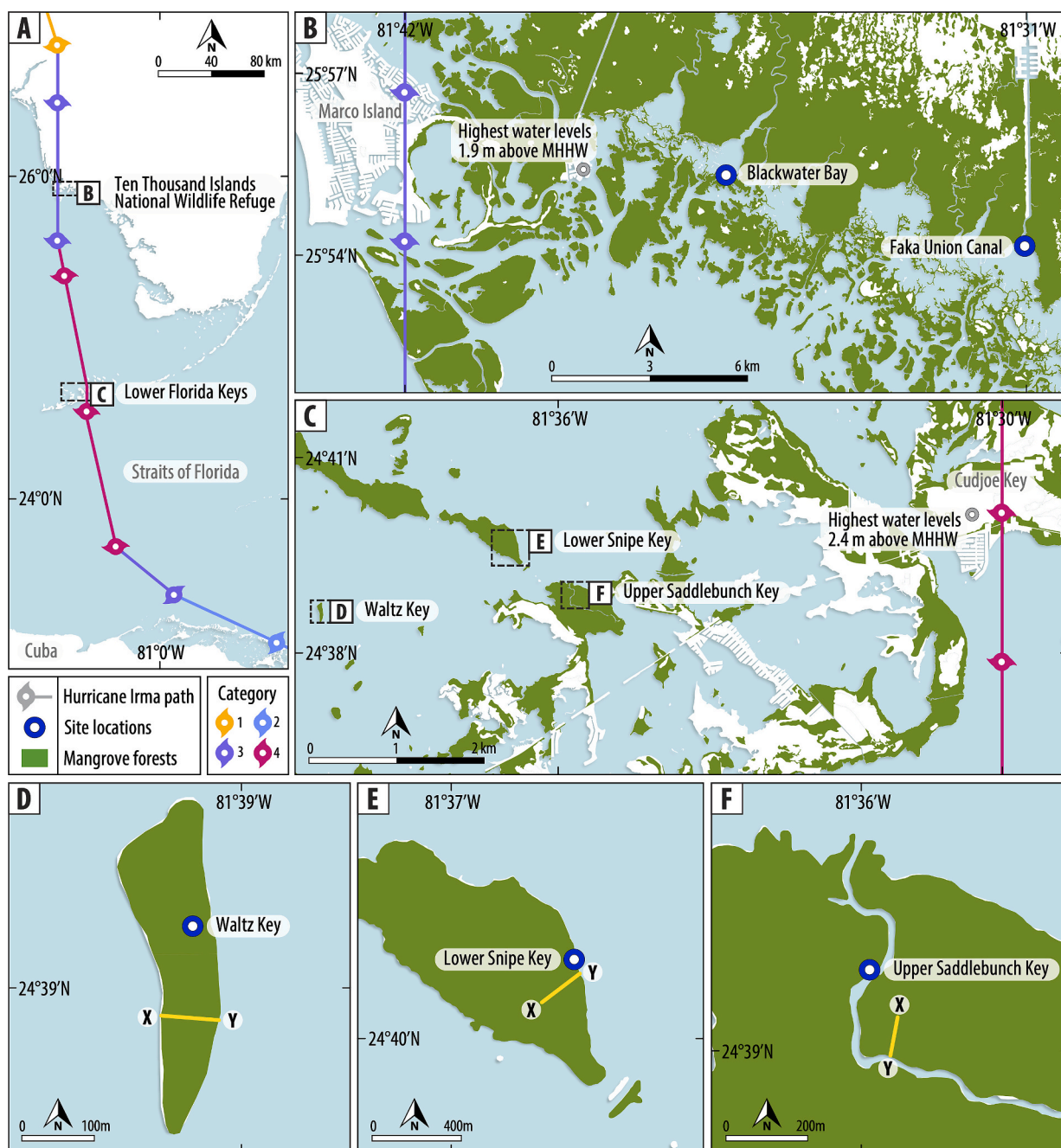


Fig. 2. (A) Path of Hurricane Irma across Florida, USA. Islands of the (B) Ten Thousand Islands National Wildlife Refuge and (C) Lower Florida Keys with locations of study sites. Site maps of (D) Waltz Key, (E) Lower Snipe Key, and (F) Upper Saddlebunch Key in the Lower Florida Keys with transects (X—Y) of sampling stations.

yet most studies of modern overwash deposits occur in temperate rather than tropical settings (e.g., Horton et al., 2009; Hawkes and Horton, 2012; Pilarczyk et al., 2016). Furthermore, discerning geologic records of overwash deposits requires an understanding of if and how such events are preserved in coastal environments (Swindles et al., 2018). If overwash deposits are not preserved in the geologic record, the record would underestimate the frequency of tropical cyclones (Lin et al., 2016). However, it is poorly understood which sedimentological, microfossil and/or biogeochemical characteristics are best preserved within geological records and how diagenesis and taphonomy can affect these characteristics over time.

Hurricane Irma was an extremely powerful hurricane that caused widespread destruction with storm surges reaching heights from 0.15 to 2.4 m above Mean Higher High Water (MHHW) (Cangialosi et al., 2018). Previous studies of Hurricane Irma's overwash deposit have described biogeochemical signatures (Breithaupt et al., 2020) as well as sedimentological and micropaleontological (foraminifera) characteristics (Martin and Muller, 2021; Mitchell et al., 2021; Wang et al., 2021) of the overwash sediments. Here, we characterize the post-depositional changes in overwash deposits from Hurricane Irma, which made landfall in southern Florida on 10 September 2017. We describe the stratigraphic, sedimentological, microfossil (foraminifera and diatoms), and geochemical (stable carbon isotopes and C/N values) indicators of Irma's overwash deposit two months and twenty-two months after the storm's landfall from five sites in the Lower Florida Keys and the Ten Thousand Islands National Wildlife Refuge, Florida. By revisiting the deposit nearly two years after the storm, we were able to identify which overwash characteristics were preserved over the study period.

2. Study area

The Florida Keys is an archipelago stretching 240 km (Hoffmeister and Multer, 1968) off the southern tip of Florida, USA, between the Atlantic Ocean and Gulf of Mexico. The Lower Florida Keys (Fig. 2C) are formed by Upper Pleistocene oolitic limestone, which comprises the upper facies of the Pleistocene Miami Limestone (Sanford, 1909; Hoffmeister and Multer, 1968; Schomer and Drew, 1982). During the Late Pleistocene, an east-west oriented oolitic sand bar formed off the southern coast of Florida (Hoffmeister and Multer, 1968, Schomer and Drew, 1982). As relative sea level fell during the onset of the Last Glacial Maximum, the retreating waters formed channels that cut normal to the oolitic sand bar and created the north-south oriented platforms on which mangroves grow today (Hoffmeister and Multer, 1968, Schomer and Drew, 1982).

The Ten Thousand Islands National Wildlife Refuge, on the Florida mainland (Fig. 2B), consists of mangrove forests growing on several meters of interbedded mangrove peats and carbonate muds and sands. These layers of sediment sit above the seaward-dipping Miocene limestone of the Tamiami Formation (Shier, 1969). Relative sea-level rise following the end of the Last Glacial Maximum created a shallow sea over the region in which a vermetid gastropod reef formed parallel to the coast (Shier, 1969). The growth of the vermetid reef created a lagoonal environment between the reef and coast. Thus, the outermost mangrove islands overlie reef barrier sediments consisting of fused vermetid tubes, reef rock, and silty sand material, while the innermost islands overlie lagoonal sediments consisting of silty sands interspersed with peaty clumps and oyster shells (Shier, 1969).

Vegetation of the mangrove islands in the Lower Florida Keys and Ten Thousand Islands is dominated by *Rhizophora mangle* (red mangrove) interspersed with *Laguncularia racemosa* (white mangrove) and *Avicennia germinans* (black mangrove) (Radabaugh et al., 2020). The Great Diurnal tidal range in the regions of Lower Florida Keys and Ten Thousand Islands is 0.69 m and 0.82 m, respectively (NOAA, 2020a, 2020b). The mangrove peats established when the rate of deglacial relative sea-level rise slowed below ~5 mm/yr at approximately 6000–4000 years ago (Willard and Bernhardt, 2011; Saintilan et al.,

2020; Khan et al., 2022).

3. Hurricane Irma

The Tropical Depression that became Hurricane Irma formed off the western coast of northern Africa on 30 August 2017 and rapidly strengthened to reach hurricane status 30 h later on 31 August. Hurricane Irma tracked west-northwest across the Atlantic Ocean and strengthened, reaching maximum intensity as a Category 5 hurricane (on the Saffir-Simpson Hurricane Wind Scale) on 5 September with winds reaching 213 km/h and minimum pressure of 914 mb (Cangialosi et al., 2018).

On 10 September, Hurricane Irma made landfall in the Lower Florida Keys as a Category 4 hurricane with maximum winds at 213 km/h and a minimum pressure of 931 mb and subsequently made landfall just south of Marco Island, FL as a Category 3 storm with maximum winds at 185 km/h and a minimum pressure of 936 mb (Cangialosi et al., 2018). By 11 September, Irma was reduced to a tropical storm over northern Florida and then to a tropical depression as the storm continued to track northwest over the United States (Carisio et al., 2018).

The Lower Florida Keys and the Ten Thousand Islands study areas were within the direct path of Irma's eyewall, which is a hurricane's most destructive region for winds and precipitation (Emanuel, 2003). In the Florida Keys, storm surge heights were highest in parts of the Lower Florida Keys. High water marks in the Lower Florida Keys, from Cudjoe Key to Big Pine Key, were as high as 1.5 to 2.4 m above MHHW (Cangialosi et al., 2018). The highest recorded water level at the National Ocean Service tide gauge in Key West, Florida, which is approximately 19 to 24 km to the southwest of study sites, reached 0.8 m above MHHW (Carisio et al., 2018). In Goodland, Florida, which is located on Marco Island and is approximately 3 to 13 km to the west of study sites, a United States Geological Survey (USGS) storm tide sensor recorded a maximum water level of 1.9 m above MHHW (Cangialosi et al., 2018).

4. Methods

4.1. Sampling design

We selected mangrove islands in the Lower Florida Keys (Lower Snipe Key, Waltz Key, and Upper Saddlebunch Key) and the Ten Thousand Islands National Wildlife Refuge, Florida (Faka Union Canal and Blackwater Bay) as sites to characterize changes in the stratigraphic, sedimentological, microfossil, and biogeochemical indicators of Hurricane Irma's overwash deposit (Fig. 2).

Four mangrove islands, two each in the Lower Florida Keys (Lower Snipe Key and Waltz Key) and the Ten Thousand Islands National Wildlife Refuge (Faka Union Canal and Blackwater Bay), were selected based on satellite imagery, aerial maps, and preliminary site reconnaissance that met the following criteria: (1) Hurricane Irma-related overwash sediments were present; (2) no site cleanup or reconstruction had been initiated; and (3) no buildings or coastal infrastructure were present to complicate inundation flow patterns. Additionally, sites were co-located with locations of ongoing work (Chappel, 2018; Khan et al., 2022), which provided baseline conditions for sites prior to the storm. We surveyed and sampled overwash sediments and the underlying substrate from five mangrove islands (including Upper Saddlebunch Key) from two months to three months (November and December 2017) following the landfall of Hurricane Irma. Sediments were re-collected at each site (along the same transects established in 2017) twenty-two months after landfall (in July 2019). We revisited the deposit nearly two years post-storm to understand how the characteristics of Irma's overwash deposit changed over the short-term.

Upper Saddlebunch Key in the Lower Florida Keys served as a control for comparison with the other study sites where overwash sediments were present. The transect on Upper Saddlebunch Key did not have Hurricane Irma-related overwash sediments present due to the

transect's interior location on the mangrove island, which provided protection from Irma's storm surge (Fig. 2F). At this site, the surficial 1 cm of sediment and organic detritus served as a comparison for the Irma deposit.

We measured local topography along cross-shore transects at each site. Along each transect, sampling stations (between 12 and 22 stations per site) were placed at evenly spaced intervals in distance (in basin mangroves with flat topography) or elevation (in fringe mangroves with an elevation gradient). The elevation of each station was related to North American Vertical Datum 1988 (NAVD88) using a Differential Global Positioning System (DGPS) or real-time kinematic (RTK) GPS. Vdatum (Yang et al., 2012) was used to convert NAVD88 to local tidal datums. Transects ranged from 50 to 255 m in distance and from -0.86 to 0.29 m NAVD88 in elevation.

During each field survey, we described the stratigraphy from a 25 mm-diameter hand gouge corer or sediment pit at each sampling station using the Troels-Smith sediment classification system (Troels-Smith, 1955). The thickness of the overwash deposit was measured once per sampling station. At one station along the transect in each of the fringe and basin mangrove environments and also at the station with peak overwash thickness, we recorded four overwash deposit thickness measurements, within an area of ~ 1 m², to monitor small-scale spatial variations. The overwash deposit was identified and differentiated from pre-Irma mangrove sediments visually in the field by colour and sediment type. At all stations where a measurable overwash deposit was present, surficial overwash sediment from a 5×5 cm area was collected for sedimentological, geochemical, and microfossil analyses. At stations where a measurable overwash deposit was not present (e.g., Upper Saddlebunch Key), the upper 1 cm of sediment was collected for analysis of the surficial sediment. Pre-overwash sediments of 1 cm thickness were also collected below the contact with the overwash deposit or surficial sediment at a similar sample volume. Each sample contained approximately 10 to 20 cm³ of sediment.

4.2. Sedimentological analyses

We measured the grain size of pre-Irma and overwash sediment samples from each station from all five mangrove islands. The samples were prepared by rinsing sediments through a 2-mm sieve to remove large roots and organic detritus. No grains larger than 2 mm were observed during sieving. Samples were digested in 30% H₂O₂ to remove any remaining organic matter and to prepare samples for grain-size measurements (Donato et al., 2009). Samples were kept at 60 °C in a hot water bath to speed the reaction (Donato et al., 2009) and triple rinsed with deionized water upon digestion completion. Grain size distributions were measured with a Malvern Mastersizer 3000 laser particle size analyzer (Donato et al., 2009). Grain size statistics were calculated using GRADISTAT software (Blott and Pye, 2001) according to the Folk and Ward (1957) method, including mean grain size, sorting, skewness, and kurtosis.

Following standard practice for paleostorm analysis (e.g., Liu and Fearn, 1993, 2000; Donnelly et al., 2001a, 2001b, 2004) we measured the loss-on-ignition of pre-Irma and overwash sediment samples from each station from all five mangrove islands as a proxy for their organic and carbonate weight percentages. Samples were dried at 105 °C for twenty-four hours to determine the dry mass of each sample (Dean Jr., 1974). Each sample's percent organic and inorganic content were measured by combusting samples in a muffle furnace at 550 °C for three hours and reweighing to obtain mass loss (Dean Jr., 1974). The loss of carbon dioxide (LOC) of each sample was measured by combusting samples in a muffle furnace at 990 °C for one and a half hours and reweighing for mass loss (Dean Jr., 1974). The LOC and the fraction of carbon dioxide in calcium carbonate (the amount of CO₂ lost during combustion at 990 °C) were used to calculate each sample's percent calcium carbonate (Dean Jr., 1974).

4.3. Geochemical analyses

We analyzed organic and bulk stable carbon isotopes ($\delta^{13}\text{C}$) as well as organic carbon and total nitrogen content ratios (C/N) of pre-Irma and overwash sediment samples from each station from all five mangrove islands. Samples for organic carbon isotopic analysis were digested in 5% HCl to remove any carbonate sediments and triple rinsed with deionized water (Vane et al., 2013; Khan et al., 2019). To prepare both the bulk and organic samples for measurements of $\delta^{13}\text{C}$, percent total nitrogen, and percent organic carbon, samples were dried at 45 °C for twenty-four hours and milled to a fine powder with a mortar and pestle (Vane et al., 2013; Khan et al., 2019). Samples were weighed into tin capsules (for bulk carbon samples) or silver and tin capsules (for organic carbon samples).

Samples were analyzed for $\delta^{13}\text{C}$ and C/N using a Flash Elemental Analyzer coupled to a Thermo Fisher Delta V isotope ratio mass spectrometer (Thermo Flash EA 1112) (Pérez et al., 2017). To calibrate for $\delta^{13}\text{C}$, a pair of working standards (glucose, 10.7 ‰ and urea, 41.3 ‰) were measured every 20 samples. The standards were initially calibrated against international absolute standards LSVEC and NIST8542. Analytical precision was 0.1‰ for organic carbon, 0.1‰ for total nitrogen, 0.1‰ for $\delta^{13}\text{C}$, and 0.15‰ for $\delta^{15}\text{N}$ (Pérez et al., 2017).

4.4. Microfossil analyses

We analyzed the microfossil assemblages (foraminifera and diatoms) of pre-Irma and overwash sediments from Waltz Key and Lower Snipe Key in the Lower Florida Keys. These two sites were selected because Irma's overwash sediments were present at all sampling stations across the transects. We selected a total of three stations from each site covering both the fringe and basin mangrove environments to capture the distribution of microfossil assemblages across the sites.

Samples obtained for foraminiferal analysis were stored in buffered ethanol upon collection (Scott et al., 2007). Samples were washed, and the 63- to 500- μm fractions were wet split into eight aliquots for counting (Scott and Hermelin, 1993; Horton and Edwards, 2006). Foraminifera species were identified and counted wet using a binocular microscope at 20 to 40 \times magnification. If possible, a total of 200 specimens in each Irma overwash sample and 100 specimens in each pre-Irma peat sample were counted to capture the range of species present in each sample. A higher number of specimens was counted in the Irma overwash samples in order to adequately quantify the greater range of species diversity observed in these samples. Dead versus alive foraminifera were not distinguished; therefore, both were included in count totals. Total counts have been used in many foraminiferal studies (e.g., Scott and Medioli, 1980; Culver et al., 1996; Hayward et al., 1999). The number of broken or fractured foraminifera tests were counted. Taxonomic classifications were based on Phleger (1965), Todd and Low (1971), Javaux and Scott (2003), and Rabien et al. (2015). Foraminifera counts are reported at the genus level due to the wide range of species present, particularly in the overwash sediment samples.

To prepare samples for diatom analysis, 1 cm³ of sediment was digested in 30% H₂O₂ to remove all organic material prior to counting (Zong and Sawai, 2015). Samples were kept at 60 °C in a hot water bath filled with deionized water to aid the digestion process, and samples were triple rinsed with deionized water upon digestion completion. An aliquot (100 to 150 μL) of each sample was placed on a coverslip and dried overnight (Hemphill-Haley, 1996; Zong and Sawai, 2015). The coverslip was mounted to a glass slide using Naphrax and labeled for counting. A maximum of 300 specimens of diatoms were counted in each sample under light microscopy at 1000 \times magnification (Zong and Sawai, 2015). Species identifications were made using Krammer and Lange-Bertalot, 1986, 1988, Krammer and Lange-Berlot, 1991a, 1991b and Witkowski et al. (2000) and classified by salinity based on global observations (Denys, 1991).

4.5. Statistical analyses

Sedimentological and geochemical datasets of pre-Irma and Irma overwash sediments at each site from 2017 and 2019 were tested for normality using a Shapiro-Wilk test (Shapiro and Wilk, 1965). Because many datasets failed the tests for normality (due to the small sample size and large range of values within the datasets), they were compared nonparametrically via Kruskal-Wallis H-tests (Kruskal and Wallis, 1952), which determines the statistical likelihood datasets originated from the same distribution based on the datasets' medians rather than means. The datasets were tested in a univariate manner in three pairs for each site [e.g., (1) Nov. 2017 pre-Irma vs. Nov. 2017 Irma; (2) Jul. 2019 pre-Irma vs. Jul. 2019 Irma; and (3) Nov. 2017 Irma vs. Jul. 2019 Irma] to determine which datasets (if any) had statistically significant differences at p -value < 0.05 . Data were analyzed using the stats package in SciPy (Virtanen et al., 2020).

Microfossil data at Waltz and Lower Snipe Keys were analyzed via hierarchical clustering to identify groups of samples across both sites with similar microfossil assemblages. Hierarchical clustering was used to reduce subjectivity and allow the algorithm to determine the number of clusters within the data. Data were clustered via Ward's Minimum Variance Linkage Algorithm based on Euclidian distance using the hierarchical linkage and clustering packages in SciPy (Virtanen et al., 2020). Principal component analysis (PCA) was also conducted on microfossil relative abundance data from both sites to determine which genera (for foraminifera) or species (for diatoms) of microfossils had the greatest influence in grouping samples by sediment type (e.g., pre-Irma or Irma) and collection date. PCA was chosen to analyze the microfossil relative abundance data because the gradient lengths of the foraminifera and diatom datasets were < 3 (2.53 and 1.23, respectively) indicating PCA was an appropriate analysis (ter Braak and Prentice, 1988). The gradient lengths were calculated using detrended correspondence analysis (DCA) in R 4.0.3 using the vegan package (Oksanen et al., 2022). The PCA analysis was conducted in R 4.0.3 using the Stats package (R Core Team, 2020). Only genera and species with the highest relative abundances ($> 5\%$ of all individuals counted) were used in the clustering, DCA, and PCA analyses for foraminifera and diatoms, respectively. Samples with < 40 specimens were not included in the clustering analysis to prevent samples with few to no specimens from distorting results (Horton and Edwards, 2006).

5. Results

We describe the results for Waltz Key (Fig. 2D) and Lower Snipe Key (Fig. 2E) from the Lower Florida Keys (Tables 1 & 2) because their results are representative of our results from the larger southern Florida region. We provide a brief description of results from Upper Saddlebunch Key. Summaries of the results from analyses for Blackwater Bay and Upper Faka Union Canal in the Ten Thousand Islands National Wildlife Refuge are shown in the Supplementary Materials.

5.1. Waltz Key

In November 2017, Irma's overwash deposit was composed of light gray carbonate silt with a trace of very fine sand and a Troels-Smith classification of $Ag_4Ga_+Dh_+$, ranging in thickness from 0.1 to 4.3 cm over the 50-m transect (Fig. 3). The deposit was thickest (4.3 cm) on the eastern edge of the island and thinned (to 0.1 cm) westward. Conversely, in July 2019, the overwash deposit was thickest on the western edge of the island (6 cm) and thinned (< 0.1 cm) eastward. The underlying pre-Irma sediments were organic-rich, heavily rooted red mangrove peats with a Troels-Smith classification of Th_2Ag_2 . In 2017, the contact between the overwash deposit and underlying sediment was sharp. In 2019, this sharp contact persisted where the overwash deposit was thickest (> 4 cm) but was less distinct elsewhere. Fallen mangrove leaves and windblown detritus were mixed into the carbonate silts, and a layer

Table 1

Summary statistics [median and interquartile range (IQR)] of sedimentological, geochemical, and microfossil data of pre-Irma and Irma overwash sediments from Waltz Key in the Lower Florida Keys collected in November 2017 and July 2019.

Waltz Key	Pre-Irma November 2017	Irma November 2017	Pre-Irma July 2019	Irma July 2019
	Median [IQR]			
Mean Grain Size (ϕ)	7.3 [0.42]	4.8 [1.1]	5.5 [2.3]	4.0 [0.65]
D10 Grain Size (ϕ)	5.0 [0.96]	2.1 [0.89]	2.2 [2.0]	1.4 [0.75]
D90 Grain Size (ϕ)	9.5 [0.57]	7.7 [0.81]	8.0 [0.71]	7.6 [0.35]
Sorting (ϕ)	1.6 [0.31]	2.0 [0.17]	2.0 [0.54]	2.4 [0.19]
Skewness (ϕ)	-0.10 [0.17]	0.26 [0.09]	-0.22 [0.53]	0.37 [0.12]
Organic Content (%)	66.2 [2.1]	21.6 [20.1]	66.4 [3.6]	41.0 [17.0]
Carbonate (%)	39.5 [3.8]	73.8 [13.8]	46.9 [8.9]	54.0 [17.2]
Organic $\delta^{13}C$ (‰)	-26.4 [0.8]	-23.4 [3.6]	-25.9 [0.2]	-25.0 [1.8]
Bulk $\delta^{13}C$ (‰)	-25.3 [0.7]	-10.5 [10.7]	-24.95 [0.6]	-20.3 [2.1]
C/N	32.4 [6.0]	73.1 [24.6]	28.2 [7.8]	34.0 [16.0]
Agglutinated Foraminifera (%)	98.0 [50.0]	0.0 [1.5]	30.0 [30.]	4.0 [11.5]
Calcareous Foraminifera (%)	4.0 [50.0]	100.0 [1.5]	70.0 [30.5]	96.0 [11.5]
Freshwater Diatom (%)	46.0 [17.5]	18.0 [13.0]	16.0 [3.5]	10.0 [11.0]
Brackish Diatoms (%)	31.0 [14.5]	24.0 [18.5]	37.0 [7.5]	50.0 [6.0]
Marine Diatoms (%)	22.0 [3.0]	50.0 [28.0]	42.0 [9.0]	50.0 [11.5]

of seagrass (*Thalassia* sp.) wrack accompanied the overwash sediments across the island in November 2017 (Supplemental Fig. 2). By July 2019, few seagrass blades remained in a highly decomposed state.

Grain size analysis showed a statistically significant difference (p -value < 0.05) between Irma's overwash deposit and pre-Irma sediments in November 2017 and July 2019 (Fig. 3 & Table 1). From November 2017 to July 2019, the mean grain size increased from a median of 4.8 to 4.0 ϕ in the overwash deposit and from a median of 7.3 to 5.5 ϕ in the pre-Irma sediments.

Loss-on-ignition analysis indicated a statistically significant difference (p -value < 0.05) in pre-Irma and Irma overwash sediments in November 2017 and July 2019. Irma's overwash sediments were composed primarily of carbonate sediments (median 73.8% in November 2017 and 54.0% in July 2019) with a lesser amount of organic material (median 21.6% in November 2017 and 41.0% in July 2019). By contrast, the underlying mangrove peat sediments were primarily composed of organic material (median 66.2% in November 2017 and 66.4% in July 2019) with a lesser amount of carbonate sediment (median 39.5% in November 2017 and 46.9% in July 2019) (Fig. 3 & Table 1).

Organic stable carbon isotopes from Irma's overwash sediments were statistically different (p -value < 0.05) from those of pre-Irma sediments in November 2017 and July 2019. In November 2017, Irma's overwash sediments were slightly heavier in $\delta^{13}C_{org}$ (median -23.4 ‰) than pre-Irma sediments (medians -26.4 ‰) (Fig. 4 & Table 1). This signal was diminished by July 2019, when $\delta^{13}C_{org}$ values of the overwash sediments became lighter (median -25.0 ‰) compared to overwash sediments collected in November 2017.

Table 2

Summary statistics [median and interquartile range (IQR)] of sedimentological, geochemical, and microfossil data of pre-Irma and Irma overwash sediments from Lower Snipe Key in the Lower Florida Keys collected in November 2017 and July 2019.

Lower Snipe Key	Pre-Irma November 2017	Irma November 2017	Pre-Irma July 2019	Irma July 2019
Median [IQR]				
Mean Grain Size (ϕ)	6.5 [0.93]	5.4 [0.65]	6.6 [1.2]	4.0 [1.3]
D10 Grain Size (ϕ)	4.4 [1.5]	3.2 [0.84]	4.7 [1.2]	1.5 [1.0]
D90 Grain Size (ϕ)	8.8 [0.48]	8.2 [0.89]	8.2 [0.56]	8.0 [0.90]
Sorting (ϕ)	1.7 [0.38]	1.9 [0.34]	1.4 [0.16]	2.4 [0.61]
Skewness (ϕ)	-0.04 [0.17]	0.11 [0.23]	-0.11 [0.22]	0.42 [0.20]
Organic Content (%)	66.0 [3.4]	15.8 [3.8]	66.8 [2.6]	46.1 [21.3]
Carbonate (%)	37.8 [4.1]	81.4 [5.0]	45.9 [12.1]	58.8 [14.2]
Organic $\delta^{13}\text{C}$ (‰)	-25.7 [1.4]	-26.5 [1.1]	-25.7 [1.7]	-25.2 [2.4]
Bulk $\delta^{13}\text{C}$ (‰)	-25.1 [1.2]	-11.2 [4.6]	-24.9 [3.3]	-20.5 [6.1]
C/N	34.8 [10.5]	84.6 [17.4]	30.3 [9.4]	34.6 [9.2]
Agglutinated Foraminifera (%)	98.0 [50.0]	1.0 [2.5]	76.0 [45.0]	7.0 [19.0]
Calcareous Foraminifera (%)	0.0 [1.0]	99.0 [2.5]	24.0 [45.0]	93.0 [19.0]
Freshwater Diatom (%)	17.0 [11.0]	9.0 [13.0]	50.0 [26.0]	14.0 [25.0]
Brackish Diatoms (%)	33.0 [4.0]	21.0 [6.5]	29.0 [10.5]	7.0 [19.5]
Marine Diatoms (%)	52.0 [8.5]	64.0 [10.0]	32.0 [21.0]	52.0 [19.5]

Bulk stable carbon isotopes from Irma's overwash sediments were significantly different (p -value < 0.05) from pre-Irma sediment values in November 2017 and July 2019. Bulk stable carbon isotopes from November 2017 showed Irma's overwash sediments were heavier in $\delta^{13}\text{C}_{\text{bulk}}$ (median - 10.5 ‰) than pre-Irma mangrove sediments (median - 25.3 ‰) (Fig. 4 & Table 1). This signal weakened in sediments analyzed from July 2019, where the median $\delta^{13}\text{C}_{\text{bulk}}$ was -20.3 ‰ for the overwash sediments and was -25.0 ‰ in the pre-Irma sediments.

C/N was significantly different (p -value < 0.05) between Irma's overwash and pre-Irma sediments in November 2017. Irma's sediments had higher C/N values (median 73.1) than their pre-Irma counterparts (median 32.4). However, this signal was reduced to the point where C/N values of Irma's overwash and pre-Irma sediments were not statistically different (p -value = 0.200) by July 2019 (medians 34.0 and 28.2, respectively).

Total foraminifera illustrated a distinct difference in assemblage, diversity, and standing crop between Irma's overwash deposit and pre-Irma sediments (Fig. 5 & Table 1). Between 230 and 250 tests per sample were identified in Irma's overwash deposit from November 2017 while 2 to 97 tests per sample were identified in pre-Irma sediments collected at the same sampling period. The pre-Irma standing crop count of 2 tests is the only sample that was below the threshold of 40 tests per sample for further statistical analyses. In November 2017, the Irma overwash deposits were dominated by a diverse, abundant calcareous assemblage with genera such as *Ammonia*, *Bolivina*, *Haynesina*, *Quinqueloculina*, and *Rosalina*. In contrast, the pre-Irma sediments were dominated by a low diversity, sparse agglutinated assemblage with genera such as *Trochammina* and *Siphotrochammina*. We identified between 173 and 243 tests per sample in Irma's overwash deposit and 100 to 145 tests per

sample in pre-Irma sediments collected in July 2019. By July 2019, agglutinated specimens were found with the diverse calcareous species in the assemblage of Irma's overwash deposit, and calcareous specimens were found with the agglutinated species in the assemblage of pre-Irma sediments. The relative abundance of broken foraminifera tests remained consistent between Irma's overwash deposit and pre-Irma sediments and sampling periods.

The hierarchical clustering and PCA analyses largely differentiated samples by pre-Irma sediment versus Irma overwash sediments and by collection date. Cluster 1 was composed entirely of 2017 Irma overwash deposit samples. Clusters 2 and 3 were composed of a mixture of 2019 pre-Irma sediment and Irma overwash deposit samples. Cluster 4 was composed of a mixture of 2017 and 2019 pre-Irma sediment samples (Fig. 6). The three pre-Irma sediment samples from July 2019 were clustered with samples of Irma's overwash deposit from July 2019 in Clusters 2 and 3 due to a relatively high number of calcareous specimens (St. 2 & 5) and lack of agglutinated specimens (St. 11) (Figs. 5 & 6).

Diatom analysis showed changes in species assemblage between Irma's overwash deposit and pre-Irma sediments (Fig. 7 & Table 1). We identified between 14 and 262 diatoms per sample in Irma overwash deposit and between 89 and 265 diatoms per sample in pre-Irma sediments collected in November 2017. Freshwater species (e.g., *Achnanthes minutissima* var. *affinis*, *Pinnularia borealis*, and *Pinnularia subcapitata*) present (>5% abundance) in pre-Irma samples but were rare (<5% abundance) or absent in the Irma overwash deposits. Although brackish species (e.g., *Amphora coffeaeformis* and *Diploneis pseudovalis*) and the allochthonous marine species *Paralia sulcata* were found in both pre-Irma and Irma sediments from 2017, the sudden presence of an anomalous marine species, *Dimeregramma fulvum*, was only observed in the overwash deposit. In samples from July 2019, we identified 7 to 61 diatoms per sample in pre-Irma sediments and 2 to 281 diatoms per sample in Irma overwash deposit. Freshwater species (e.g., *Navicula erifuga* and *Gyrosigma acuminatum*) were again present in pre-Irma samples but became rare or absent in the Irma overwash deposit. However, brackish and marine species (e.g., *Amphora subacutiuscula*, *Gammatophora oceanica*, *Melosira moniliformis*, and *Navicula microdigitradiata*) were present in both Irma overwash and pre-Irma sediments. Four samples did not meet the threshold of 40 diatoms: two samples were from pre-Irma sediment, and two samples were from Irma's deposit. One sample was collected in 2017, and three samples were collected in 2019. Hierarchical clustering and PCA analysis were unable to differentiate samples by sediment type (pre-Irma versus Irma) or collection date (Fig. 8).

5.2. Lower Snipe Key

In November 2017, Irma's overwash deposit was a light gray carbonate silt with a trace of very fine sand and a Troels-Smith classification of $\text{Ag}_4\text{Ga}_1\text{Dh}_+$ ranging in sediment thickness from 0.1 to 5.5 cm over the 250 m transect (Fig. 9). The deposit was thickest (5.5 cm) at the mangrove fringe-basin boundary and thinned (0.1 cm) on either side of this boundary. By July 2019, the deposit remained thickest (4.5 cm) at the fringe-basin boundary and appeared to be mixed with an organic mud. The deposit had thickened on either side of the point of maximum thickness before thinning to ~0.1 cm in the fringe and basin. Underlying Irma's overwash deposit was autochthonous organic-rich, heavily rooted red mangrove peat with a Troels-Smith classification of Th_2Ag_2 . The contact between the overwash deposit and the underlying mangrove peats remained sharp between sampling periods, particularly where the deposit was thickest (>2 cm). Fallen mangrove leaves and other wind-blown detritus were mixed in with the carbonate silts, and a layer of seagrass (*Thalassia* sp.) wrack accompanied the overwash sediments in the fringe of the mangrove island in November 2017 (Supplemental Fig. 2). By July 2019, very few blades of seagrass remained in a highly decomposed state.

Grain size analysis was able to significantly differentiate (p -value

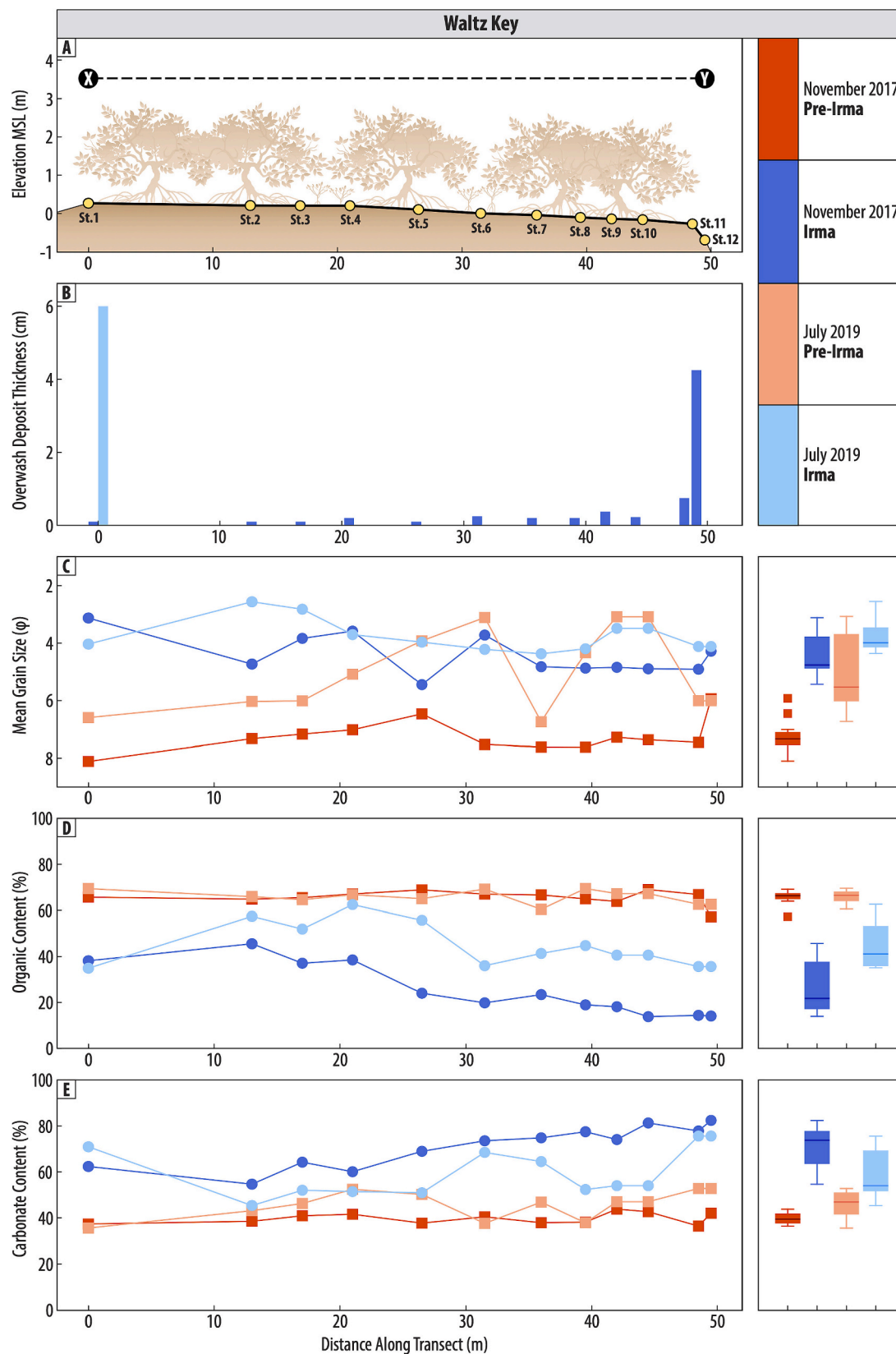


Fig. 3. Sedimentological results of pre-Irma mangrove peats and Irma overshaw sediments from November 2017 and July 2019 at Waltz Key in the Lower Florida Keys. (A) Elevation and location of stations along transect, (B) thickness of Irma deposit, (C) mean grain size (ϕ), (D) organic content (%), and (E) carbonate content (%). Box plots indicate median, interquartile range (IQR), Q1 (Q3) + (-) IQR*1.5, and outliers.

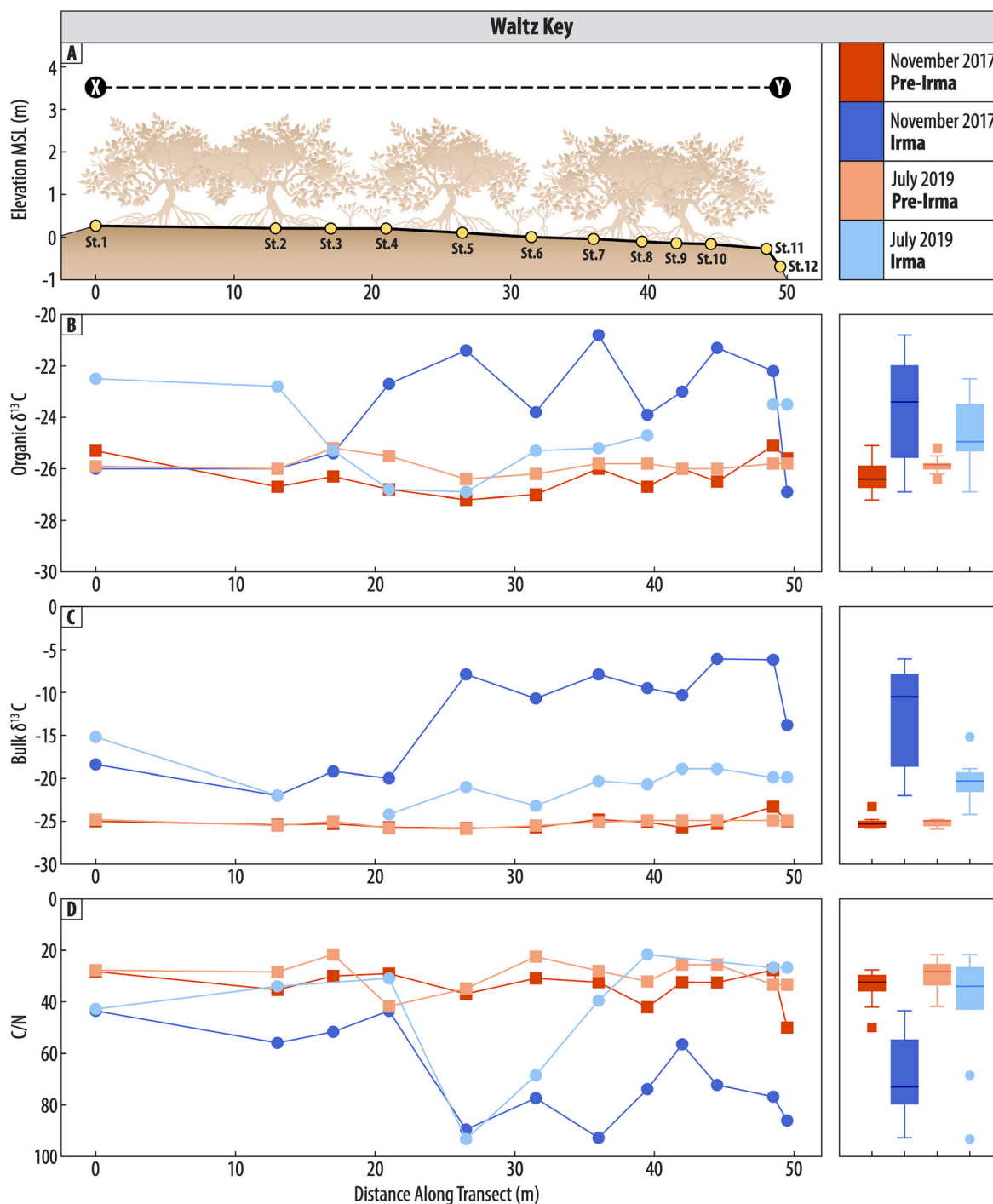


Fig. 4. Stable carbon and C/N geochemistry results of pre-Irma mangrove peats and Irma overshaw sediments from November 2017 and July 2019 at Waltz Key in the Lower Florida Keys. (A) Elevation and location of stations along transect, (B) organic $\delta^{13}\text{C}$ (‰), (C) bulk $\delta^{13}\text{C}$ (‰), and (D) $C_{\text{organic}}/N_{\text{total}}$. Box plots indicate median, interquartile range (IQR), Q1 (Q3) + (–) IQR*1.5, and outliers.

<0.05) Irma's overshaw deposit from the underlying pre-Irma mangrove sediments in both November 2017 and July 2019 (Fig. 9 & Table 2). Mean grain size increased from a median of 5.4 to 4.0 ϕ in the overshaw deposit and remained constant (median 6.5 to 6.6 ϕ) in the pre-Irma sediments from November 2017 to July 2019.

Loss-on-ignition analysis showed a significant difference (p -value <0.05) in pre-Irma sediment and Irma's overshaw deposit from November 2017 and July 2019. In 2017, the overshaw deposit was predominantly composed of carbonate sediments (median 81.4%) with a lesser component of organic material (median 15.8%) (Fig. 9 &

Table 2). In contrast, the pre-Irma sediments were largely organic (median 66.0%) with a smaller portion of carbonate material (median 37.8%). Although this signal was diminished by July 2019, the overshaw deposit (median 46.1% organic and 58.8% carbonate) remained statistically different from the underlying mangrove peat (median 66.8% organic and 45.9% carbonate).

Organic $\delta^{13}\text{C}$ signatures were unable to distinguish Irma's overshaw deposit from underlying pre-Irma sediments in November 2017 (p -value = 0.481) or July 2019 (p -value = 0.233). While $\delta^{13}\text{C}_{\text{org}}$ values of the overshaw deposit (median = 26.5 ‰) were slightly lighter than those of

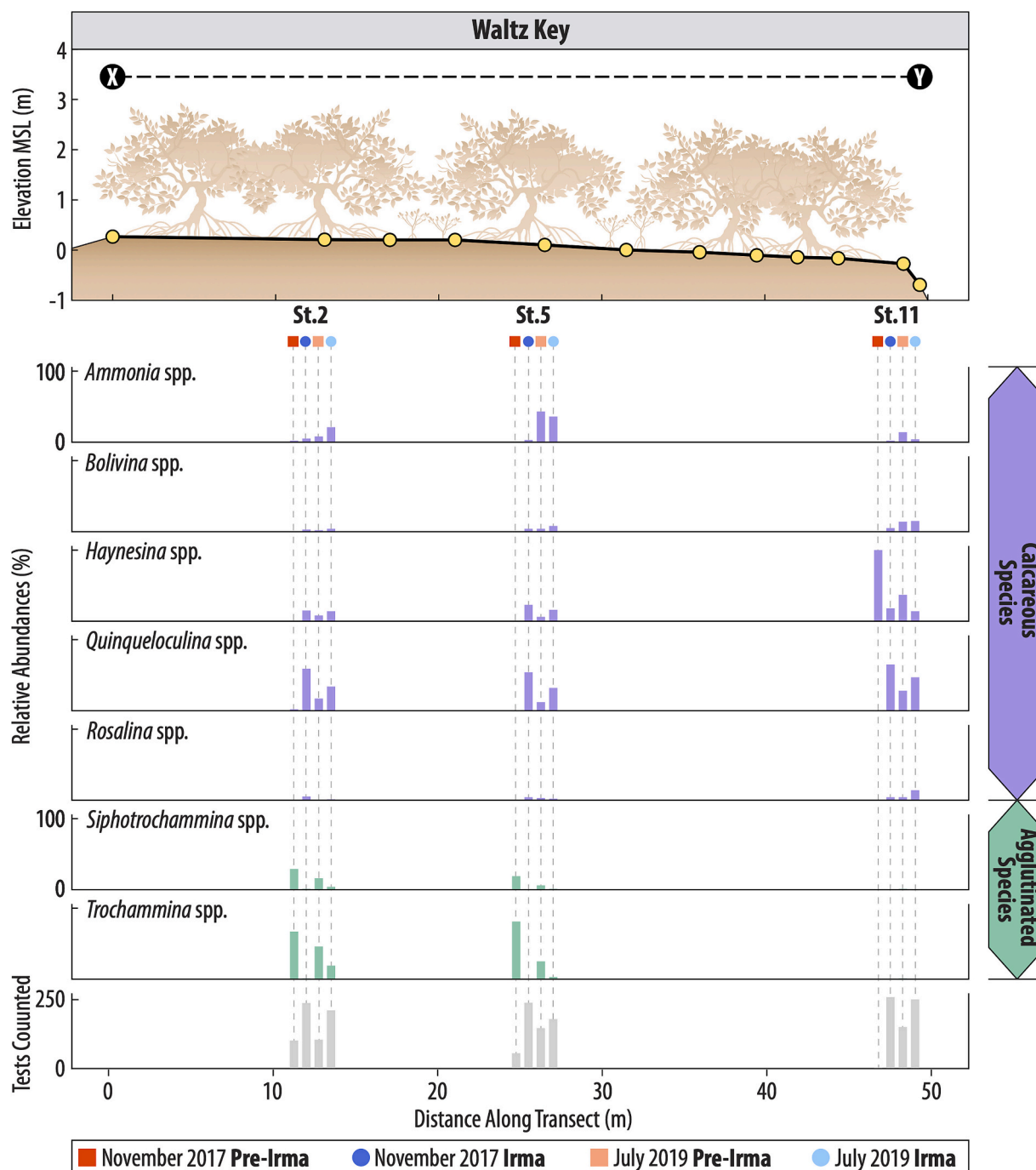


Fig. 5. Foraminifera relative abundances (%) from three stations along the Waltz Key transect. Elevation of stations and genus relative abundances (%) per sample. Order of columns for each station from left to right is (i) pre-Irma sediments from November 2017, (ii) Irma overshaw sediments from November 2017, (iii) pre-Irma sediments from July 2019, and (iv) Irma overshaw sediments from July 2019. Agglutinated species are colored in green, and calcareous species are colored in purple. (For interpretation of the references to colour in this figure legend, the reader is referred to the web version of this article.)

the pre-Irma sediments (median – 25.7 ‰) in November 2017, the values were too similar to be considered significantly different (Fig. 10 & Table 2). Median $\delta^{13}\text{C}_{\text{org}}$ of Irma's overshaw deposit became heavier (–25.2 ‰) by July 2019 but was not significantly different than the $\delta^{13}\text{C}$ of underlying pre-Irma sediments (–25.7 ‰).

Bulk $\delta^{13}\text{C}$ values were able to differentiate (p-value <0.05) Irma's overshaw deposit from pre-Irma sediments in November 2017 and July 2019. Irma overshaw sediments were heavier in $\delta^{13}\text{C}$ (median – 11.2 ‰) than pre-Irma sediments (median – 25.1 ‰) (Fig. 10 and Table 2). Although the overshaw sediments became lighter in $\delta^{13}\text{C}$ (median – 20.5 ‰) by July 2019, they remained statistically differentiable from

pre-Irma sediments (median – 24.9 ‰).

Organic carbon to total nitrogen ratios (C/N) were significantly different (p-value <0.05) between Irma's overshaw deposit and pre-Irma sediments in November 2017 but not in July 2019 (p-value = 0.121). C/N values were higher in Irma's overshaw deposit (median 84.6) in November 2017 than in pre-Irma sediments (median 34.8). However, by July 2019, C/N values of Irma's overshaw deposit (median 34.6) were reduced enough to not be statistically different from pre-Irma sediments (median 30.3). The inclusion of the outlier value from the pre-Irma sediments from 2017 at Station 5 (C/N 215) did not influence the statistical interpretations.

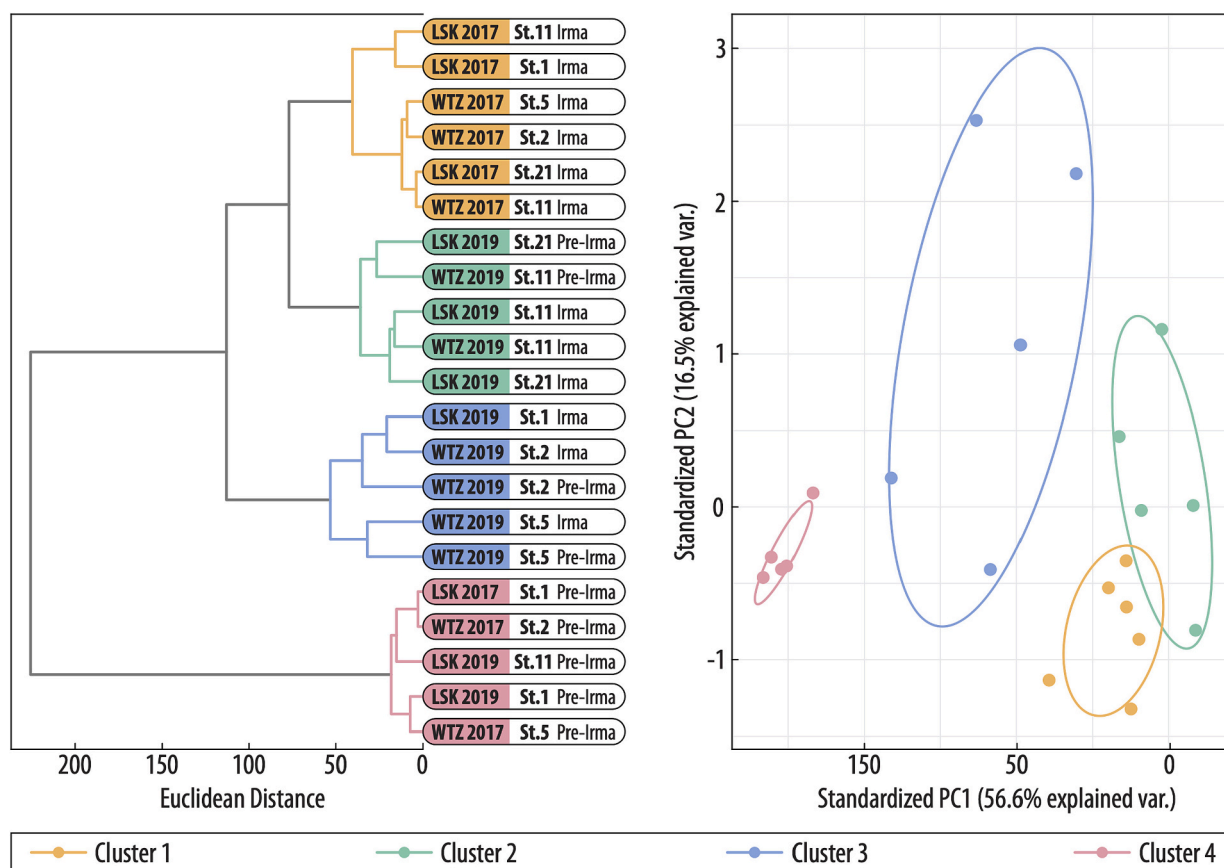


Fig. 6. (A) Clustering and (B) PCA diagrams based on relative foraminifera genus abundances in pre-Irma and Irma overshaw sediment samples from stations at Waltz and Lower Snipe Keys in November 2017 and July 2019.

Total foraminifera showed a clear division in assemblage, diversity, and standing crop between Irma's overshaw deposit and the underlying pre-Irma sediments (Fig. 11 & Table 2). We identified between 86 and 271 and 0 to 105 tests per sample in Irma's overshaw deposit and pre-Irma sediments collected in November 2017, respectively. In samples collected from July 2019, we identified 63 to 200 and 44 to 101 tests per sample within Irma's overshaw deposit and pre-Irma sediments, respectively. The 2017 pre-Irma sediment sample at St. 21 contained zero foraminifera tests, but by 2019 had 44 predominately comprised of species from the *Bolivina* and *Haynesina* genera. In November 2017 and July 2019, the foraminifera assemblage in Irma's overshaw deposit was composed primarily of diverse and abundant calcareous genera including *Ammonia*, *Bolivina*, *Haynesina*, *Quinqueloculina*, and *Rosalina*. Conversely, the assemblage of the pre-Irma sediments was dominated by sparse, low diversity, agglutinated genera including *Trochammina* and *Siphotrochammina*. By July 2019, a small number of agglutinated specimens were counted within the overshaw deposit, particularly in the mangrove basin (St. 1), and a small number of calcareous specimens were counted in the underlying mangrove peat, particularly in the mangrove fringe (St. 21). The relative abundance of broken foraminifera tests in samples did not vary across Irma's overshaw deposit and pre-Irma sediments or sampling date.

Clustering and PCA analyses separated samples by sediment type (pre-Irma and Irma) and collection date. Two pre-Irma sediment samples collected in November 2017 did not exceed the 40 specimen per sample threshold for further statistical analyses. Cluster 1 was composed entirely of 2017 Irma overshaw deposit samples. Clusters 2 and 3 were composed of a mixture of 2019 pre-Irma sediment and Irma overshaw deposit samples. Cluster 4 was composed of a mixture of 2017 and 2019 pre-Irma sediment samples (Fig. 6). One pre-Irma sediment sample from July 2019 (St. 21) was clustered with Irma overshaw deposit samples

from the same sampling date due to its relatively high abundances of calcareous genera.

Diatom analysis found a mixture of assemblages in Irma's overshaw deposit and the underlying pre-Irma sediments (Fig. 12 & Table 2). We identified 65 to 269 diatoms per sample in Irma's overshaw deposit and 52 to 249 diatoms per sample in pre-Irma sediments collected in November 2017. All samples from November 2017 contained brackish and marine species, but an absence of a freshwater species at >5% abundance. The brackish species *Amphora coffeaeformis* and the marine species *Stenoneis obtuserostrata* were observed in high abundances (28 and 46%, respectively) in the Irma overshaw samples. From sediments collected in July 2019, we identified between 5 and 267 diatoms in Irma's overshaw deposit and 14 and 31 diatoms per sample in pre-Irma sediments. In July 2019, both pre-Irma sediments and Irma's overshaw deposit contained a mixture of freshwater (e.g., *Melosira varians*), brackish (e.g., *Amphora coffeaeformis*), and marine (e.g., *Cocconeis krammeri*) species. The presence of *Paralia sulcata* was observed in high abundance in the Irma overshaw samples from Stations 1 (41%) and 11 (40%). However, it should be noted only one sample of Irma's overshaw deposit collected in July 2019 contained enough specimens to exceed the 40-specimen threshold for statistical analyses. Therefore, while slight increases in brackish and marine diatom species were found in Irma overshaw sediments over pre-Irma sediments, clustering and PCA analyses were unable to group any of these samples by sediment type (pre-Irma versus Irma) or collection date (Fig. 8).

5.3. Upper Saddlebunch Key

In November 2017 and July 2019, surficial sediments included a carbonate silt with traces of fine sand (Troels-Smith classification Ag₄Ga₊Dh₊) of 1 cm thickness that pinched out into a light dusting

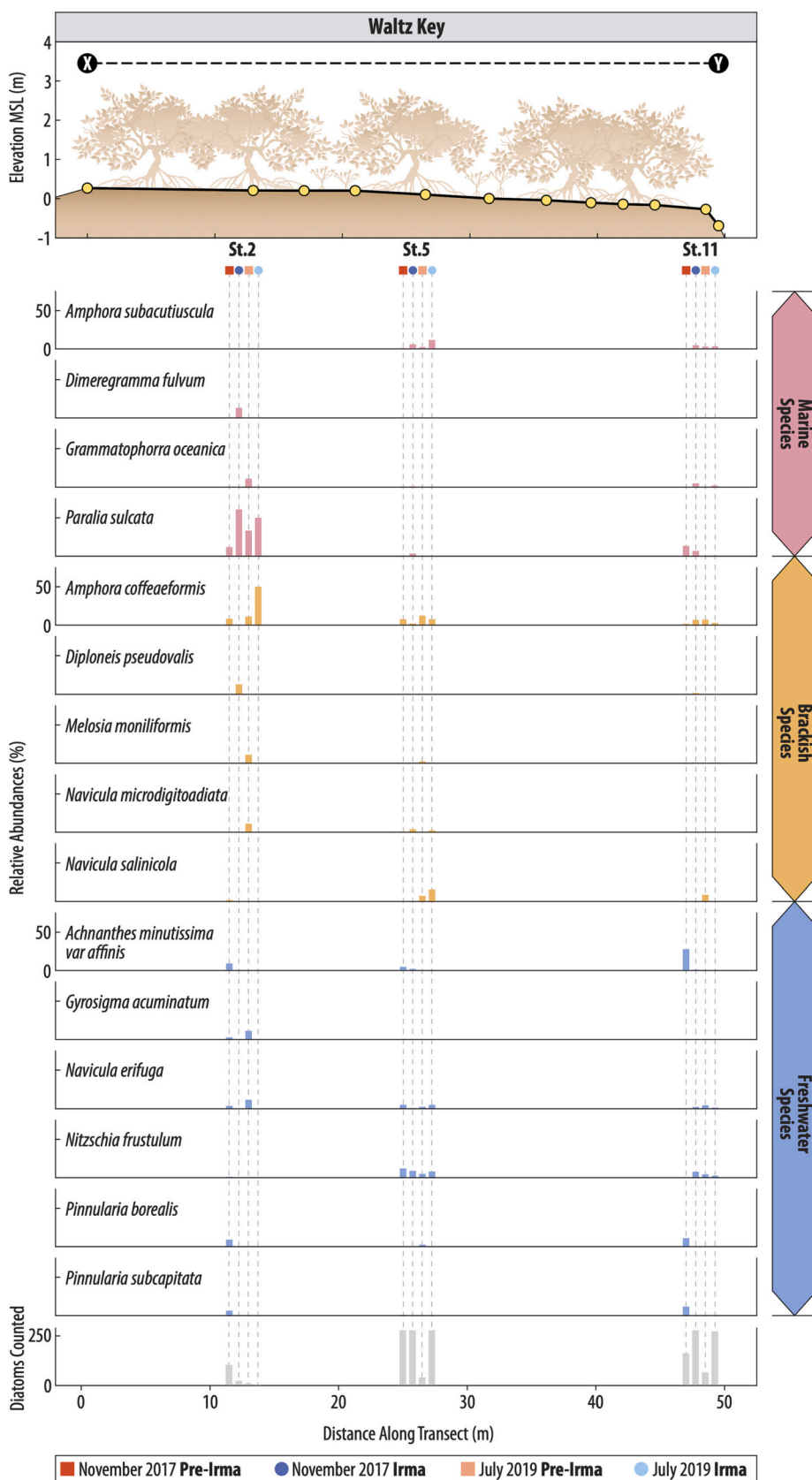


Fig. 7. Diatom relative abundances (%) from three stations along the Waltz Key transect. Elevation of stations and relative abundances of diatom species. Order of columns for each station from left to right is (i) pre-Irma sediments from November 2017, (ii) Irma overwash sediments from November 2017, (iii) pre-Irma sediments from July 2019, and (iv) Irma overwash sediments from July 2019. Freshwater species are in blue, brackish species are in yellow, and marine species are in pink. (For interpretation of the references to colour in this figure legend, the reader is referred to the web version of this article.)

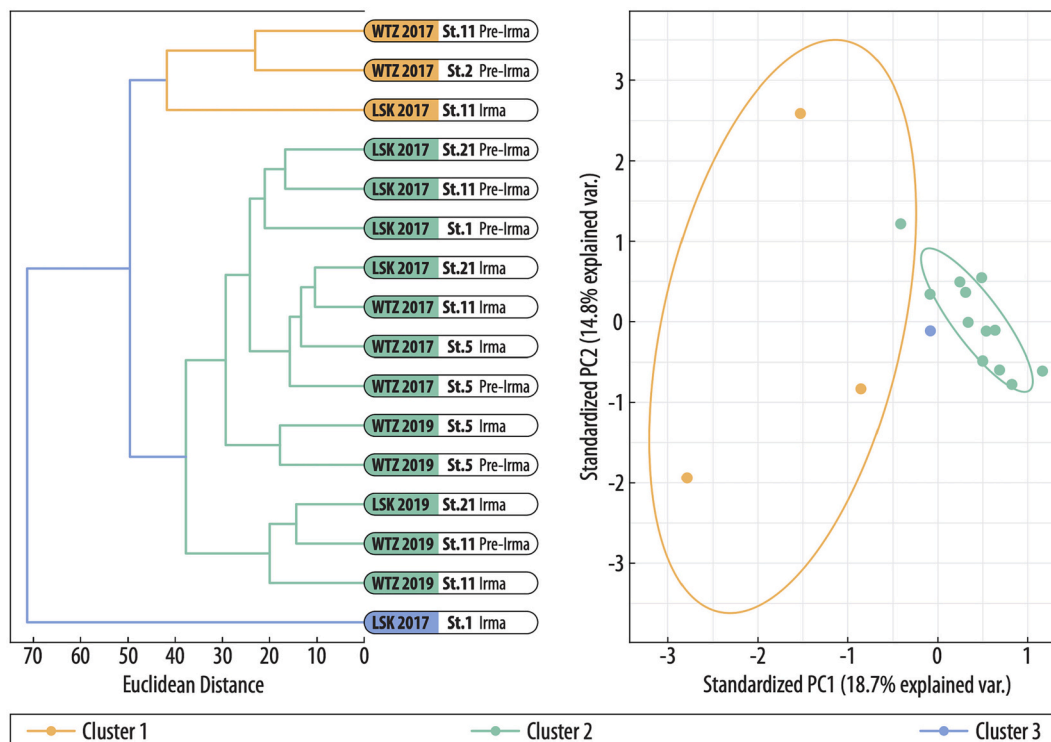


Fig. 8. (A) Clustering and (B) PCA diagrams based on relative diatom species abundances in pre-Irma and Irma overwash sediment samples from stations at Waltz and Lower Snipe Keys in November 2017 and July 2019.

over the 7 m of the transect closest to the tidal creek. It is assumed that this carbonate silt originates from tidal wave action given its proximity to the tidal creek. Over the remaining 86 m of transect in the basin of the mangrove island, surficial sediments were comprised of a heavily rooted red mangrove peat (Troels-Smith classification $Th_2Ag_2Dh_+$).

Mean grain size of the surficial sediments in November 2017 ranged from 2.9 ϕ in the carbonate silt to 7.2 ϕ in the mangrove peats (Supplemental Table 1). Similarly in July 2019, mean grain size ranged from 4.2 ϕ in the carbonate silt to 6.9 ϕ in the mangrove peats.

Organic content of the surficial sediments ranged from 17.4% in the carbonate silt to 74.1% in the mangrove peat in November 2017 (Supplemental Table 1). In July 2019, organic content increased in the carbonate silt to 45.8% while remaining at 73.0% in the mangrove peats. Conversely, carbonate content was higher in the silts along the tidal creek ranging from 82.4% in 2017 to 59.8% in 2019. Carbonate contents were lower in the mangrove peats ranging from 28.2% in 2017 and 33.9% in 2019.

Organic stable carbon isotope values of the surficial sediment ranged from -27.7 to -21.4 ‰ across the transect in 2017 and remained consistent ranging from -26.9 to -24.6 ‰ across the transect in 2019 (Supplemental Table 1). Bulk stable carbon isotope values, in 2017, were heavier in the carbonate silts adjacent to the tidal creek (-7.2 ‰) compared to the mangrove peats further inland (-27.3 ‰). In 2019, $\delta^{13}C_{bulk}$ values were more consistent across the transect ranging from -22.8 ‰ in the carbonate silts to -27.2 ‰ in the mangrove peats. In 2017, C/N values varied across the transect independently of sediment composition, ranging from 31 to 79. Similarly in 2019, C/N values ranged from 29 to 108 across the transect.

6. Discussion

6.1. Stratigraphy and deposit taphonomy

Tropical cyclone deposits have been identified in the geologic record as allochthonous nearshore and beach sediments interbedded in

autochthonous coastal sediments in low-energy salt marsh or lagoonal environments (e.g., Liu and Fearn, 1993, 2000; Donnelly et al., 2001a; McCloskey and Liu, 2012). At all sites where overwash sediments were present, Hurricane Irma's overwash deposit was composed of allochthonous sediments originating from the carbonate-rich, shallow marine environment surrounding the Lower Florida Keys and Ten Thousand Islands National Wildlife Refuge. The overwash deposit was found overlying autochthonous mangrove peats. At our control site of Upper Saddlebunch Key, surficial sediments were composed of autochthonous mangrove peats across the majority of the transect with tidally emplaced carbonate silts found along the edge of the tidal creek.

Overwash sediments from tropical cyclones are often found as landward-thinning, fan-shaped deposits (Liu and Fearn, 1993, 2000; Donnelly et al., 2001a, 2001b, 2004). Hurricane Irma's overwash deposit was similarly found to be landward thinning along transects. The thickness of Irma's overwash deposit ranged by site and across sites from several centimeters (≤ 11 cm) in thickness to a dusting (< 0.1 cm). Wang et al. (2021) study of the sedimentary characteristics of Hurricane Irma's overwash deposit in sink holes from Big Pine Key in the Lower Florida Keys also found that overwash sediments thinned landward from a maximum thickness of 5 cm.

Hurricane Irma's overwash deposit changed in thickness between the time of deposition in 2017 and when the site was revisited in 2019. At sites where the overwash deposit was originally (in November 2017) observed to be thin (< 0.1 cm), the overwash sediments were no longer preserved or were preserved in the form of carbonate nodules on the floor of the mangrove forest or in clumps under the prop roots of *Rhizophora mangle* by July 2019 (Supplemental Fig. 2E). Williams and Flanagan (2009) made comparable observations of Hurricane Rita's overwash deposit when it was revisited seventeen months after the original survey. Williams and Flanagan (2009) found Rita's overwash deposit had been redistributed and was greatly reduced in thickness in locations where the deposit was unvegetated. Contrarily, in densely vegetated areas, they found sediment thicknesses were maintained (Williams and Flanagan, 2009).

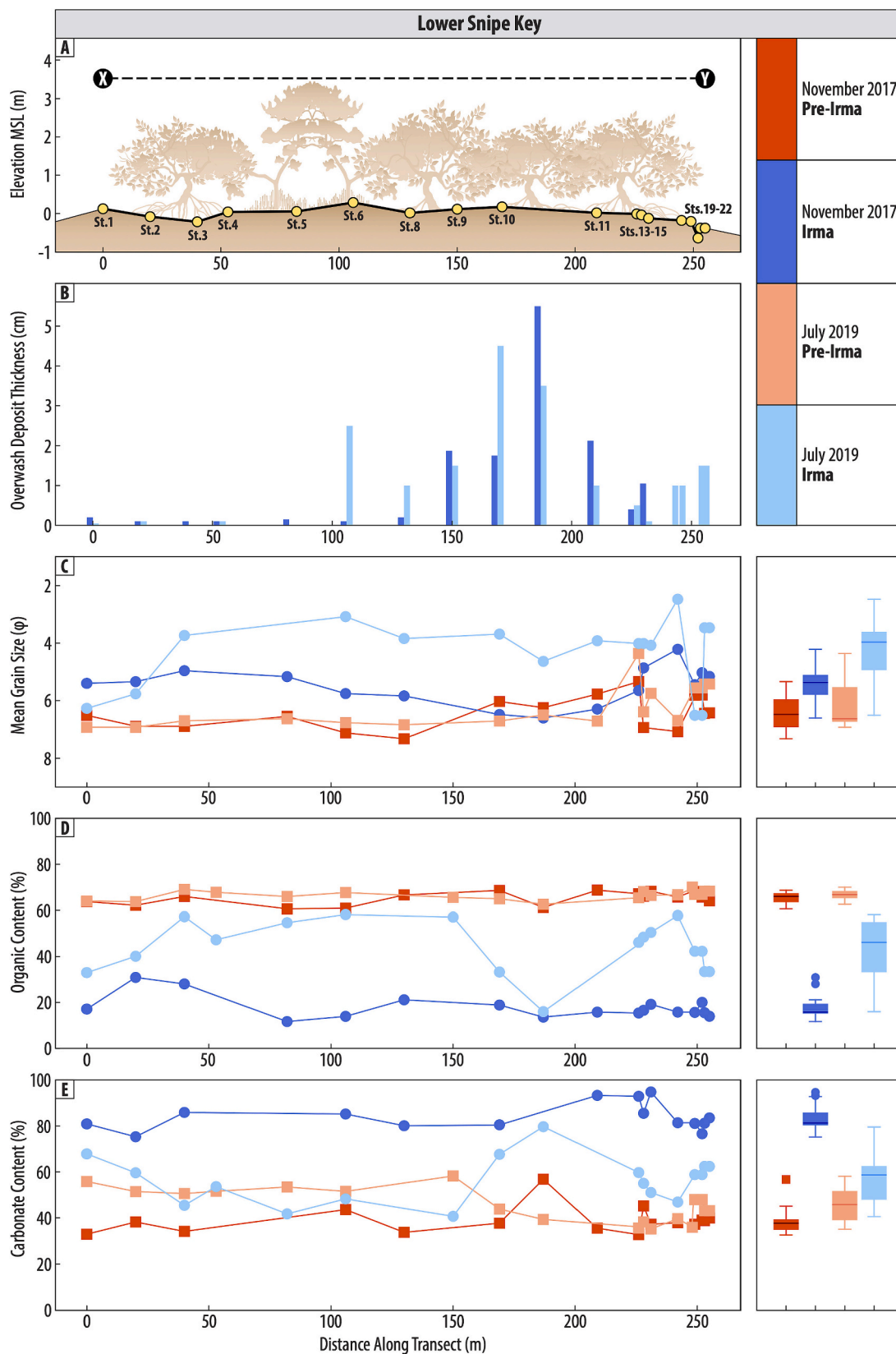


Fig. 9. Sedimentological results of pre-Irma mangrove peats and Irma overshaw sediments from November 2017 and July 2019 at Lower Snipe Key in the Lower Florida Keys. (A) Elevation and location of stations along transect, (B) thickness of Irma deposit, (C) mean grain size (ϕ), (D) organic content (%), and (E) carbonate content (%). Box plots indicate median, interquartile range (IQR), Q1 (Q3) + (-) IQR*1.5, and outliers.

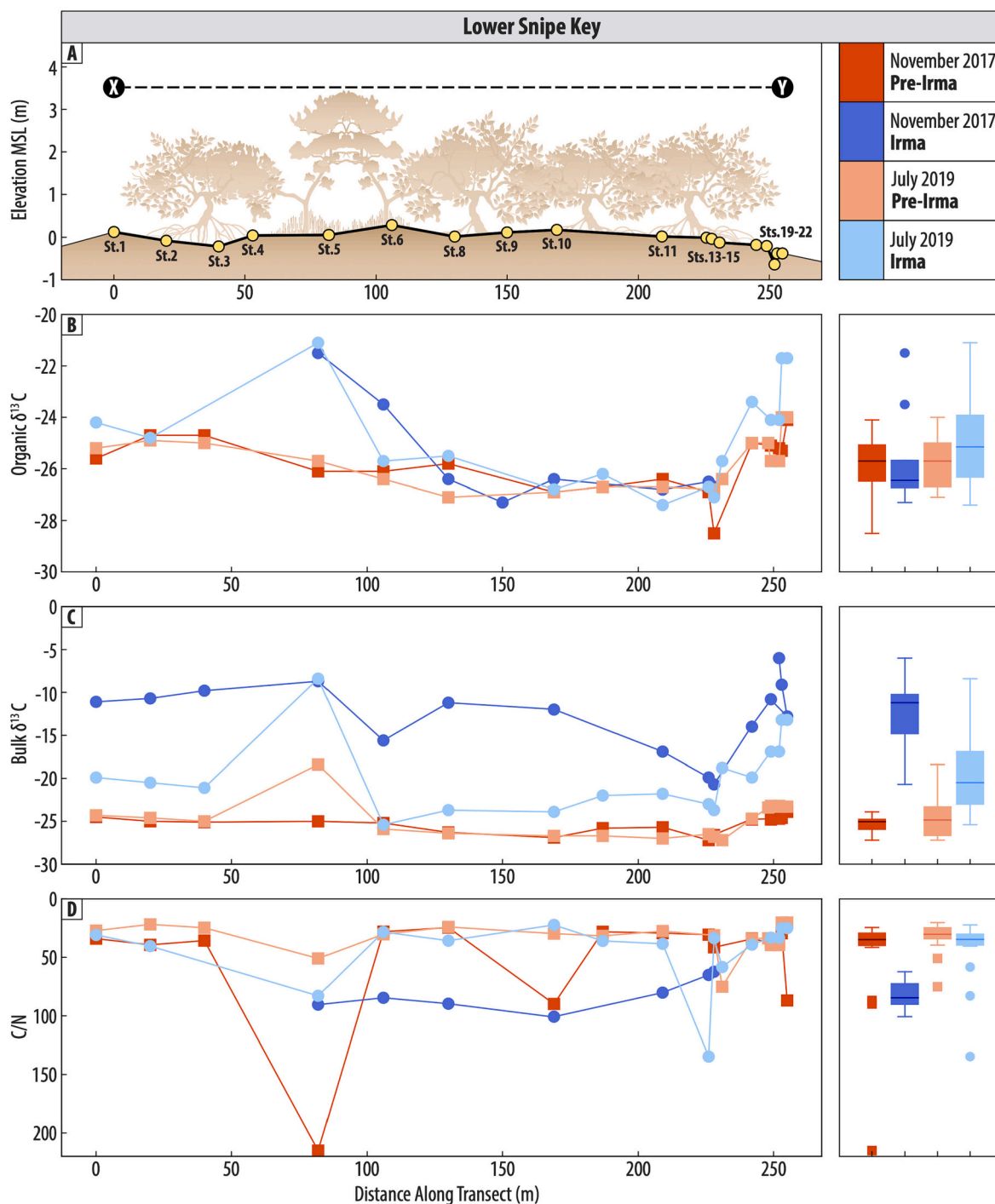


Fig. 10. Stable carbon and C/N geochemistry results of pre-Irma mangrove peats and Irma overshaw sediments from November 2017 and July 2019 at Lower Snipe Key in the Lower Florida Keys. (A) Elevation and location of stations along transect, (B) organic $\delta^{13}C$ (‰), (C) bulk $\delta^{13}C$ (‰), and (E) $C_{organic}/N_{total}$. Box plots indicate median, interquartile range (IQR), Q1 (Q3) + (–) IQR*1.5, and outliers.

The stratigraphy of tropical cyclone overshaw deposits commonly have a sharp contact with the underlying pre-storm sediments (e.g., Donnelly et al., 2001b, 2004; Horton et al., 2009). Similarly, the contact between Hurricane Irma’s overshaw deposit and underlying mangrove peats was sharp (<0.1 cm) (Supplemental Fig. 2) in most locations, particularly at stations where the deposit was at its greatest thickness (>2 cm). However, at stations on the fringes of mangrove islands (e.g., Waltz Key Station 12), the contact between the overshaw deposit and underlying mangrove peats appeared gradational (>0.1 cm). Hong et al. (2018) similarly noted sharp contacts between the Tropical Cyclone Pam

overshaw deposit and underlying sediments at all sites in Vanuatu except for sites located closest to the shoreline. Williams and Flanagan (2009) documented a similar preservation of Hurricane Rita’s overshaw deposit and the sharp contact with underlying woodland and salt marsh sediments in coastal Louisiana when they surveyed the Rita deposit six weeks and nineteen months post-storm. The sharp contact underlying Hurricane Irma was maintained from November 2017 to July 2019 at stations with a measurable (>0.1 cm) deposit.

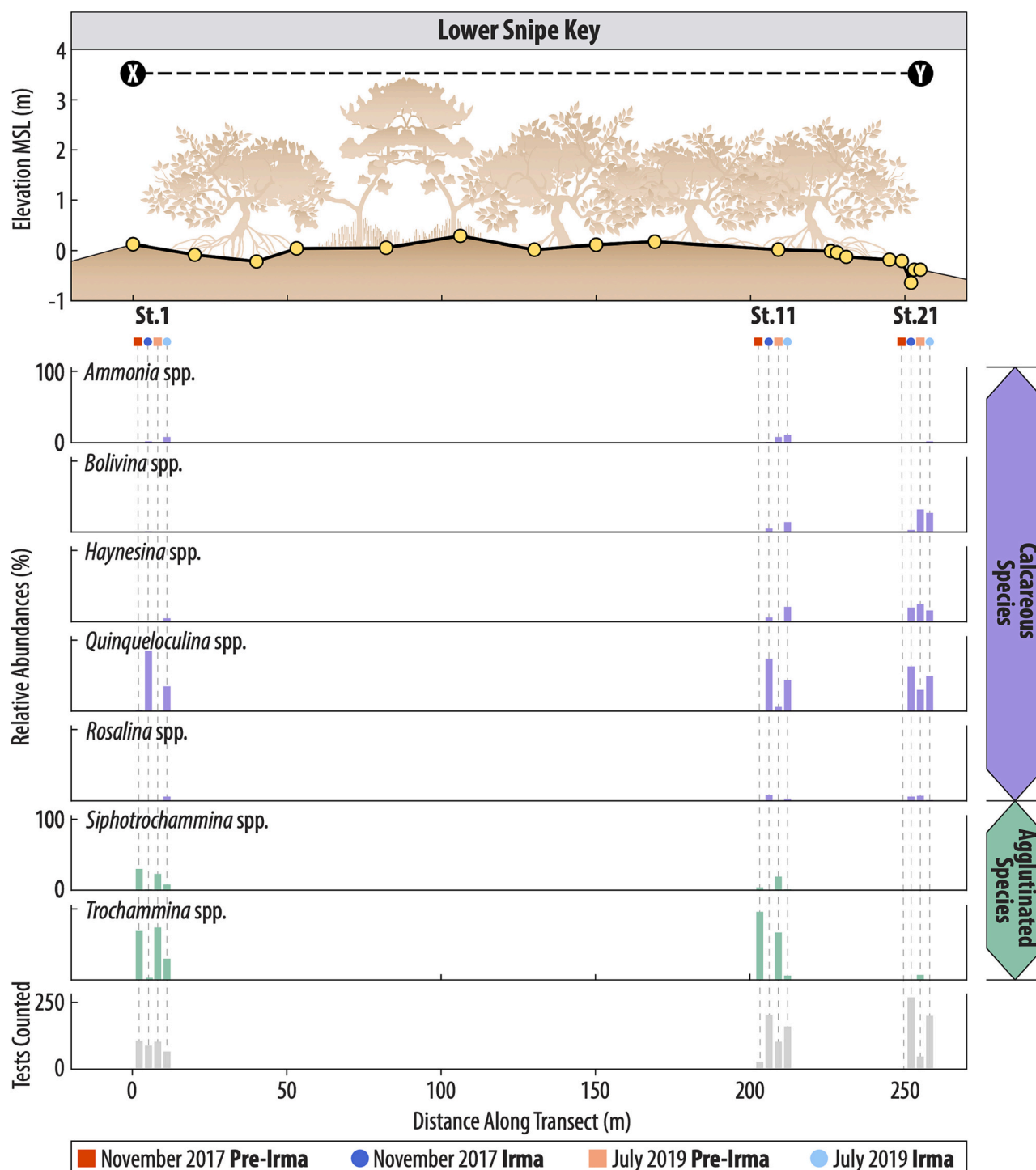


Fig. 11. Foraminifera relative abundances (%) from three stations along the Lower Snipe Key transect. Elevation of stations and genus relative abundances (%) per sample. Order of columns for each station from left to right is (i) pre-Irma sediments from November 2017, (ii) Irma overshoot sediments from November 2017, (iii) pre-Irma sediments from July 2019, and (iv) Irma overshoot sediments from July 2019. Agglutinated species are colored in green, and calcareous species are colored in purple. (For interpretation of the references to colour in this figure legend, the reader is referred to the web version of this article.)

6.2. Sedimentological analyses

Numerous studies have investigated the sedimentological features of modern overshoot deposits and have noted the comparatively coarser grain size of overshoot sediments (e.g., Williams, 2010; Soria et al., 2017; Hong et al., 2018). Soria et al. (2017) found overshoot deposits from Typhoon Haiyan throughout the northwestern coastal plains of the Philippines. Typhoon Haiyan's overshoot sediments were larger in grain

size across transects compared to the underlying pre-Haiyan soils (Soria et al., 2017). Hurricane Irma's overshoot deposit was composed of carbonate silts and sands that had a coarser mean grain size ($5.0 \pm 0.79 \phi$ across sites) than the underlying mangrove peats ($6.7 \pm 0.68 \phi$ across sites) at most sites where the deposit was present (e.g., excluding Upper Saddlebunch Key). The exception was the site at Blackwater Bay in the Ten Thousand Islands, where mean grain size of the underlying mangrove peats was larger than other sites ($5.6 \pm 0.94 \phi$) and not

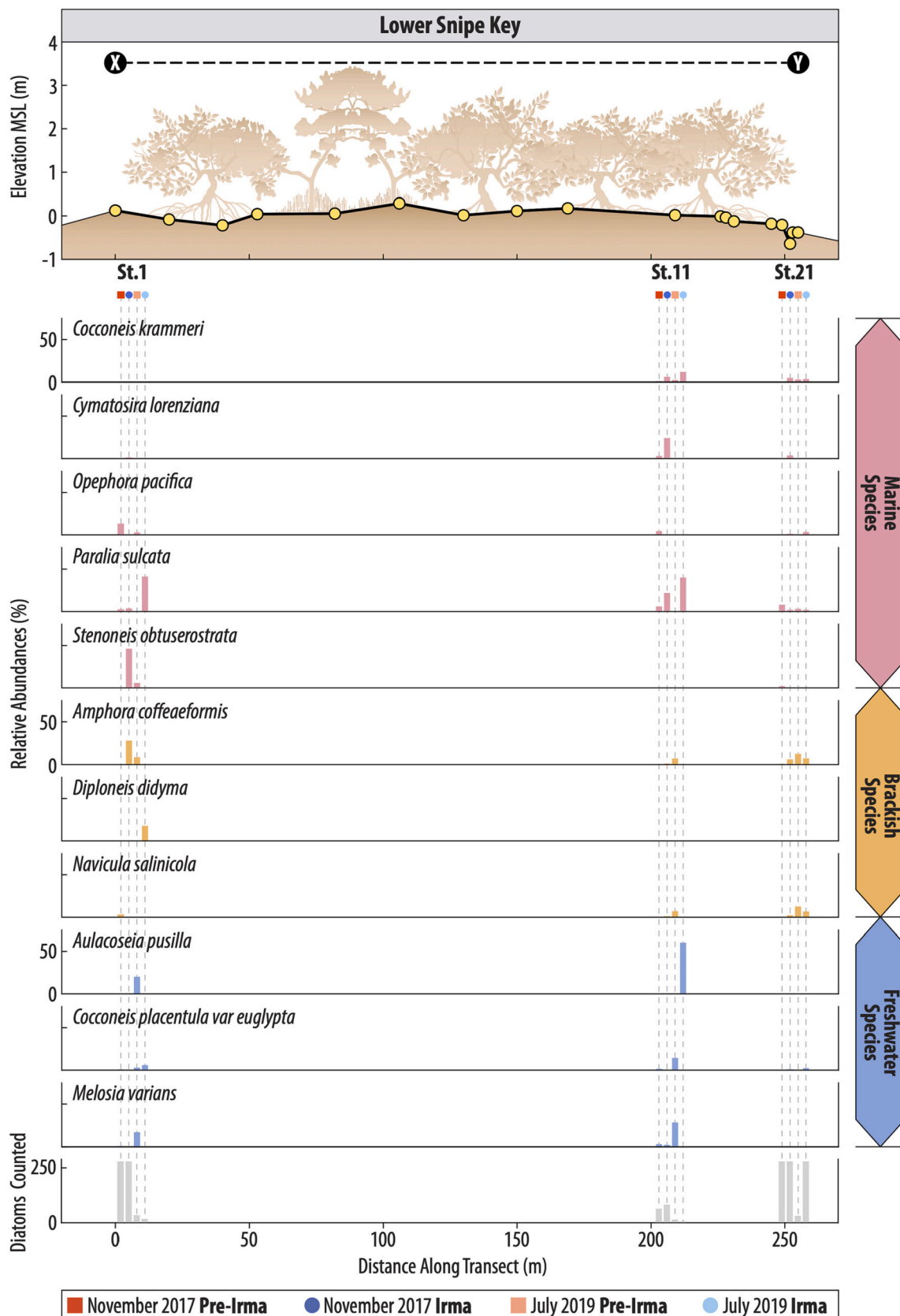


Fig. 12. Diatom relative abundances (%) from three stations along the Lower Snipe Key transect. Elevation of stations, relative abundances of diatom species, and specimen counts per sample. Order of columns for each station from left to right is (i) pre-Irma sediments from November 2017, (ii) Irma overwash sediments from November 2017, (iii) pre-Irma sediments from July 2019, and (iv) Irma overwash sediments from July 2019. Freshwater species are in blue, brackish species are in yellow, and marine species are in pink. (For interpretation of the references to colour in this figure legend, the reader is referred to the web version of this article.)

distinct from Irma's overwash sediments ($5.0 \pm 0.45 \phi$). Sediments in the Ten Thousand Islands region have a larger grain size, ranging from coarse silts to very fine sands (5.0 to 3.0ϕ) (Scholl, 1963), given their proximity to the open bay, between-island channels, and the mangrove island belt. Sediments from the Florida Bay region of the Lower Florida Keys are comparatively finer-grained with very fine ($>4.0 \phi$) to fine ($>3.0 \phi$) grained sediments (Ginsburg, 1956). The coarser sediments of the Ten Thousand Islands explain the larger mean grain size of the pre-Irma sediments at our site in Blackwater Bay, which is located along a large channel within the bay.

The carbonate content of Irma's overwash sediments ($67.8 \pm 20.7\%$ across sites) was higher than the underlying peats ($33.7 \pm 11.0\%$ across sites). Higher carbonate contents were also found in Irma's overwash deposit at sites in the Everglades National Park and at Big Pine Key in the Lower Florida Keys (Breithaupt et al., 2020; Wang et al., 2021). The sediment source for Hurricane Irma's overwash deposit included carbonate muds and sands from the Florida Bay and carbonate- and organic-rich muds and quartz sands from waters surrounding the Ten Thousand Islands National Wildlife Refuge (Ginsburg, 1956; Scholl, 1963). Martin and Muller (2021), on the other hand, found Irma's overwash sediments originating from Estero Bay were composed of quartz sands, reflecting the local source material of the region north of the sites studied here.

Overwash deposits can have several other defining sedimentological characteristics related to their texture and grading (e.g., Schwartz, 1975; Leatherman and Williams, 1977). For example, previously documented modern overwash deposits have been shown to display fining- and coarsening-upward trends in grain size (e.g., Wang and Horwitz, 2007; Switzer and Jones, 2008; Phantuwoongraj et al., 2013). Inundation from storm surges that is slow moving and sustained can create fining-upward sequences, as energy from the storm surge decreases and allows finer particles to fall out of suspension with time. Conversely, coarsening-upward sequences can occur if higher energy conditions are restored by subsequent waves or return flow (Morton et al., 2007). However, no such trends were found in Irma's overwash deposit in this study or noted in other sedimentological studies of the deposit (Martin and Muller, 2021; Wang et al., 2021). As Irma's overwash sediments were deposited as massive muds and sands, it can be assumed their deposition was rapid as a traction load (e.g., Morton et al., 2007; Williams, 2009, 2010).

Overwash deposits from tropical cyclones have a characteristically lower organic content than the surrounding sediments due to their source material originating from a more minerogenic environment than the organic-rich back-barrier environments in which they are deposited (e.g., Donnelly et al., 2004; Scileppi and Donnelly, 2007; Reese et al., 2008). Hurricane Irma's overwash deposit had a lower organic content ($19.8 \pm 9.07\%$) compared to the underlying mangrove peats ($59.4 \pm 14.6\%$) among nearly all sites where the overwash deposit was present. The site at Faka Union Canal was the only site with an overwash deposit where the organic contents of the Irma and pre-Irma sediments were indistinguishable (p -value >0.05) by July 2019. The overwash deposit at Faka Union Canal in July 2019 was only present in the form of scattered carbonate nodules and pockets of carbonate sediments under prop roots (similar to what is shown in Supplemental Fig. 2E). Breithaupt et al. (2020) also found one site in Everglades National Park, which experienced minimal marine influence, where Hurricane Irma's overwash deposit had a lower organic content than underlying peats. Wang et al. (2021) similarly found Irma's overwash deposit had less total organic matter than underlying sediments in sink holes on Big Pine Key in the Lower Florida Keys, and Martin and Muller (2021) found Irma's quartz sands had a higher percent inorganic content than the underlying sediments in a back-barrier lagoon in Estero Bay.

By July 2019, differences in the mean grain size and organic content of Irma's overwash deposit from underlying pre-Irma mangrove peats remained larger at sites in the Lower Florida Keys than in the Ten Thousand Islands National Wildlife Refuge (Supplemental Table 4) and in areas of the mangrove islands where the deposit was thickest. This

includes the fringe and basin-to-fringe boundary of the mangroves. Similar findings were made by Williams and Flanagan (2009) regarding Hurricane Rita's overwash deposit, who saw overwash sediments redistributed from high elevations to lower elevations with denser vegetation and wetter conditions.

Following a tropical cyclone, if accommodation space allows, it is assumed normal back-barrier sedimentation that occurred prior to the storm event resumes post-storm, preserving the overwash event into the geologic record (Donnelly et al., 2001a, 2001b, 2004; Donnelly and Webb III, 2004). This assumption is supported by the gradational contact between the overwash deposits and overlying low-energy sediments observed in sediment cores (e.g., Liu and Fearn, 1993, 2000; Donnelly et al., 2001a, 2001b, 2004). In July 2019, Irma's overwash deposit was covered by a thin (<1 mm) layer of newly deposited organic mud at sites in the Ten Thousand Islands National Wildlife Refuge, suggesting a resumption of normal low-energy deposition. Wang et al. (2021), who surveyed sites at Big Pine Key seven months post-storm, also found evidence of post-storm sediments that matched the sedimentology (e.g., smaller grain size and higher organic content) of pre-storm sediments suggesting a resumption of background sedimentation.

6.3. Geochemical signatures

Organic $\delta^{13}\text{C}$ in conjunction with C/N signatures have the potential to indicate the provenance of overwash sediments in low-energy coastal environments (e.g., Lamb et al., 2007; Lambert et al., 2008; Das et al., 2013). The organic isotopic signatures of coastal sediments help distinguish sources of terrestrial versus marine organic matter which constitute the sediments (i.e., autochthonous vegetation versus allochthonous phytoplankton and algae) (e.g., Emery et al., 1967; Meyers, 1994; Khan et al., 2015b). The primary sources of organic carbon in mangrove forests include mangrove litter, sea grasses, and marine particulate organic matter (POM) (Kristensen et al., 2008). Reported values of $\delta^{13}\text{C}_{\text{org}}$ in mangrove litter (i.e., leaves and branches) in southern Florida mangroves are relatively light, ranging from -32 to -27 ‰ (Fourqurean and Schrlau, 2003; He et al., 2021). On the other hand, allochthonous marine organic matter have heavier values of $\delta^{13}\text{C}_{\text{org}}$; reported values for *Thalassia* sp. leaves range from -11 to -8 ‰ (Fourqurean and Schrlau, 2003; Campbell and Fourqurean, 2009), and values for POM range from -24 to -18 ‰ depending on proximity to the coast (Lamb and Swart, 2007).

The $\delta^{13}\text{C}_{\text{org}}$ signature of Hurricane Irma's overwash deposit (-25.0 ± 2.3 ‰ across sites) did not differ from that of pre-Irma mangrove sediments (-26.0 ± 0.9 ‰ across sites) at sites where Irma's overwash deposit was present (Fig. 13). These results are not consistent with previous studies of the organic geochemical signature of overwash deposits associated with storm surges (e.g., Lambert et al., 2008; Das et al., 2013). Lambert et al. (2008) used positive organic $\delta^{13}\text{C}$ and $\delta^{15}\text{N}$ excursions in a core from coastal Lake Shelby, Alabama, to identify episodes of storm-surge flooding of the lake. Similarly, Das et al. (2013) used organic $\delta^{13}\text{C}$, $\delta^{15}\text{N}$, and C/N indicators to identify occurrences of marine inundation from storm surges in coastal lakes along the Gulf of Mexico over the last 4 ka. Our study sites differ from previous studies in that southern Florida is a carbonate-rich environment in a fully marine setting. Hurricane Irma's overwash deposit is composed primarily of inorganic carbonate sediments, which are documented as having heavily enriched values of $\delta^{13}\text{C}$ ranging from -4 to 4 ‰ (Scalan and Morgan, 1970; Boutton, 1991). When the inorganic fraction is removed from samples, the organic carbon within Irma's overwash sediments is not distinguishable from that of pre-Irma sediments.

Bulk (including inorganic carbon) $\delta^{13}\text{C}$ was successful at differentiating the carbonate-rich signal of the overwash sediments from the organic-rich underlying mangrove peats at all sites where the overwash deposit was present except for the site in the Upper Faka Union Canal in the Ten Thousand Islands National Wildlife Refuge (Fig. 13). The high-carbonate content of the overwash deposit resulted in high $\delta^{13}\text{C}_{\text{bulk}}$

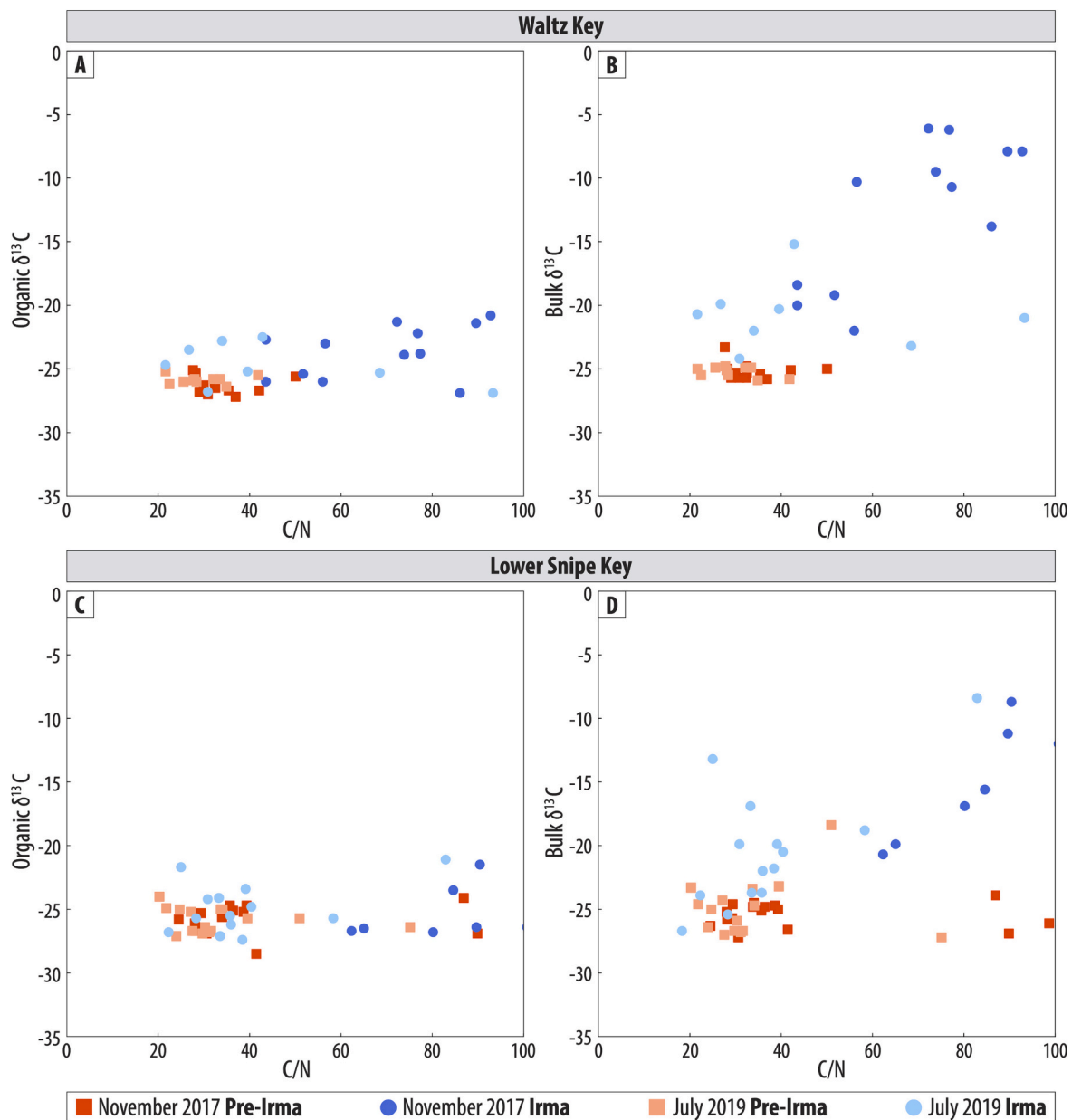


Fig. 13. Stable carbon isotopic and C/N results from Waltz Key: (A) organic $\delta^{13}\text{C}$ vs C/N and (B) bulk $\delta^{13}\text{C}$ vs C/N; and Lower Snipe Key: (C) organic $\delta^{13}\text{C}$ vs C/N and (D) bulk $\delta^{13}\text{C}$ vs C/N.

values of -12.9 ± 5.8 ‰ across sites where the overwash deposit was present (-21.9 ± 3.1 ‰ at Upper Faka Union Canal). $\Delta^{13}\text{C}_{\text{bulk}}$ values of the underlying mangrove peats were relatively low at -24.9 ± 2.3 ‰ across sites where the overwash deposit was present (-27.3 ± 1.8 ‰ at Upper Faka Union Canal). $\Delta^{13}\text{C}_{\text{bulk}}$ is seldom utilized to determine the provenance of coastal sediments as the $\delta^{13}\text{C}$ of inorganic carbon are characteristically lower than those of organic carbon and can complicate the interpretation of results (Khan et al., 2015a).

C/N ratios in conjunction with $\delta^{13}\text{C}_{\text{org}}$ measurements are useful for differentiating terrestrial versus marine provenances and providing information on the degree of diagenesis in coastal sediments (Lamb et al., 2006; Khan et al., 2015a). Aquatic organic matter tends to have higher levels of bulk N compared to terrestrial organic matter and, thus, comparatively lower C/N ratios (Lamb et al., 2006; Khan et al., 2015a). C/N values were useful in differentiating Irma's overwash deposit from underlying mangrove peats in November 2017 at sites in the Lower Florida Keys (Fig. 13). The overwash sediments had higher C/N values

(73 ± 17 across sites) compared to the underlying mangrove peats (38 ± 16 across sites). The C/N values were likely elevated by the presence of the seagrass wrack that was found accompanying the overwash sediments throughout sites in the Lower Florida Keys. Seagrasses have relatively high values of C/N, with a mean of ~ 20 but as high as 50, compared to other marine organic matter (e.g., Duarte, 1990; Fourqurean et al., 1992; Khan et al., 2015a). However, by July 2019, the C/N values of overwash sediments (43 ± 26 across sites) from sites in the Lower Florida Keys were undifferentiable from those of the underlying mangrove peats (32 ± 11 across sites) (Fig. 13). Although Fourqurean and Schrlau (2003) also note an initial increase in C/N values during the decomposition of *Thalassia testudinum* leaves in Florida Bay, they found an overall net zero change in C/N values over a year of observations. C/N values were not indicative of a difference between Irma's overwash deposit and underlying mangrove peats in December 2017 or July 2019 at sites in the Ten Thousand Islands National Wildlife Refuge. No seagrass wrack was noted at these sites during site surveys.

6.4. Microfossil analyses

Foraminifera in overwash deposits have been shown to have distinct assemblages from underlying pre-storm sediments that are more abundant, more diverse, and more likely to be of marine origin than their pre-storm counterparts (e.g., Hippensteel et al., 1999; Hawkes and Horton, 2012; Pilarczyk et al., 2016). Pilarczyk et al. (2016) used foraminifera assemblages to characterize the overwash deposit from Typhoon Haiyan at sites in the Leyte Gulf, Philippines. The foraminiferal assemblage of Haiyan's overwash deposit contained a high abundance of calcareous specimens and a high species diversity indicating a marine origin for the sediment (Pilarczyk et al., 2016). The foraminiferal assemblage in Irma's overwash deposit likewise consisted of diverse and abundant calcareous taxa. While the limited number of samples analyzed for foraminifera in this study may omit some of the spatial variability in assemblages across site (e.g., Murray and Alve, 2000; Morvan et al., 2006; Milker et al., 2015), the samples that were analyzed show a clear differentiation between samples from pre-Irma sediment and Irma's overwash deposit. In November 2017, the foraminifera within the overwash deposit were $98.5 \pm 2.1\%$ calcareous specimens across sites with 14 to 28 species identified per sample, largely from the genera of *Ammonia*, *Bolivina*, *Haynesina*, *Quinqueloculina*, and *Rosalina*. The underlying mangrove sediments had a uniform and sparse assemblage with $98 \pm 2\%$ agglutinated foraminifera that consisted of *Trochammina inflata* and *Siphotrochammina lobata* species.

Clustering and PCA analyses showed Irma's overwash sediments could be differentiated from underlying pre-Irma sediments based on the abundance of calcareous versus agglutinated specimens within samples (Fig. 6). This differentiation was greatest in samples from November 2017 due to high numbers of *Quinqueloculina* spp. and *Rosalina* spp. specimens in Irma's overwash deposit versus the exclusive presence of *Trochammina inflata* and *Siphotrochammina lobata* specimens in pre-Irma sediments. The foraminiferal assemblage of Hurricane Irma's overwash deposit did not change from November 2017 to July 2019. However, samples from July 2019 displayed mixing between Irma overwash deposit and pre-Irma sediments as shown in Clusters 2 and 3 (Fig. 6).

Other studies of Hurricane Irma's overwash deposit found comparable results in foraminiferal assemblages to this study. Wang et al. (2021) found an increase in the diversity of marine foraminifera species in Irma's overwash sediments from a sink hole on Big Pine Key. Pre-Irma sediments were dominated by *Ammonia* spp. or *Quinqueloculina* spp., while Irma's overwash sediments contained an abundance of *Ammonia* spp., *Elphidium* spp., *Quinqueloculina* spp., and *Triloculina* spp. (Wang et al., 2021). Irma's overwash deposit from Estero Bay contained calcareous foraminifera (Martin and Muller, 2021).

Taphonomic analysis of foraminifera can be used to determine the alteration and preservation potential of foraminifera tests in intertidal sediments through time (e.g., Berkeley et al., 2009; Pilarczyk et al., 2014, 2016). However, foraminifera within Irma's overwash deposit appeared unaltered through time with no change in the relative abundance of fractured foraminifera, perhaps due to the limited time length of our study. Infaunal foraminifera species or reworked sediments are an additional process by which foraminifera assemblages can be skewed over time (Berkeley et al., 2007). Our foraminifera assemblages suggest some reworking of sediments may have occurred over the 2-year study period, where pre-Irma samples incorporated higher abundances of marine calcareous foraminifera by 2019.

Diatoms have previously been used to identify overwash deposits via anomalous changes in assemblages (e.g., Parsons, 1998; Horton and Sawai, 2010; Wang et al., 2019). Parsons (1998) used diatoms to identify an overwash deposit from Hurricane Andrew in a Louisiana salt marsh pond. Hurricane Andrew's diatom assemblage showed the overwash sediments had a composite nature with components from freshwater, brackish, and marine origins (Parsons, 1998). The diversity of diatom species in Hurricane Andrew's overwash deposit increased over pre-Andrew pond sediments. Similarly, Wang et al. (2019) looked at

diatoms in modern samples from a multitude of wetland and aquatic environments, including a salt marsh, plant bog, river, and bay, to determine the provenance of an 8-cm sand layer interbedded in peat sediments in coastal Alabama that is thought to be from the landfall of a hurricane in 1772. A combination of freshwater, brackish, and marine diatoms were identified within the sand layer indicating multiple sediment sources from simultaneous marine inundation and terrestrial flooding from a storm (Wang et al., 2019).

As in previous studies, the diatom assemblage of Irma's overwash deposit displayed a mixture of freshwater (e.g., *A. pusilla*), brackish (e.g., *A. coffeaeformis*), and marine (e.g., *S. obtuserostrata*) diatom species. However, only samples from Waltz Key displayed an increase in assemblage diversity in the Irma overwash deposit compared to pre-Irma sediments, consistent with the overwash deposit of Hurricane Andrew (Parsons, 1998). At Waltz Key, samples with >40 specimens counted had an average of 40 (± 4) species identified compared to 27 (± 10) species in pre-Irma sediments. At Lower Snipe Key, species diversity was consistent between pre-Irma and Irma sediments.

While our study shows qualitative differences in the diatom assemblages of Irma's overwash deposit and pre-Irma sediments (i.e., marine species being dominant or in higher relative abundances in Irma sediments over pre-Irma sediments), these differences were not captured by clustering analyses (Fig. 8). The lack of a clear clustering of diatom assemblages between Irma's overwash sediments against underlying mangrove peats in statistical analyses may reflect the influence of several local environmental factors including elevation, salinity, and substrate (Admiraal, 1984; Vos and de Wolf, 1993; Desianti et al., 2019) and the small sampling size of this study. Differences in diatom assemblages between pre-Irma and Irma samples may be driven by changes in environmental factors over a short distance (McIntire, 1978). Hong et al. (2021) found site-specific variability in diatom assemblages at four sites in Willapa Bay, Washington when showing the use of diatoms to reconstruct relative sea-level in the region. This variability originated from the multitude of environmental factors that can control diatoms (Hong et al., 2021).

Studies have been conducted to document the geographic and temporal distributions of diatom species in Florida Bay, and two of the main conclusions drawn from these studies were (1) salinity was the dominant environmental factor contributing to the clustering of diatom samples in the region; and (2) distributions of diatoms varied seasonally, seemingly due to changes in temperature and salinity (Frankovich et al., 2006; Wachnicka et al., 2010). Wachnicka et al. (2010) documented diatom assemblages from freshwater, mangrove, and marine sites throughout Florida Bay and found, while the assemblages of freshwater and marine sites were distinct, the assemblages from mangrove sites had taxa typical of the freshwater and marine sites. Additionally, inter-site variability was attributed to seasonal changes in water quality (Wachnicka et al., 2010). Our sampling times of November 2017 and July 2019 fell within typical periods of minimum and maximum annual salinity, respectively, within Florida Bay (Kelble et al., 2007). Additionally, both the Waltz Key and Lower Snipe Key transects experience daily marine influence through tidal inundation. Therefore, it is reasonable to hypothesize the variation created by seasonal salinity changes in addition to the mixed assemblages observed in mangrove environments contributed to complex diatom assemblages found at our sites. A study looking at the spatial and temporal distribution of modern diatom species with respect to local environmental factors in southern Florida mangrove forests is needed to shed light on how to better statistically analyze and interpret perturbations in diatom assemblages observed following a storm.

7. Conclusion

We analyzed the stratigraphic, sedimentological, geochemical, and microfossil characteristics of Hurricane Irma's overwash deposit in southern Florida mangroves (Fig. 14). We tracked changes in the overwash deposit's characteristics compared to those of underlying pre-Irma

Characteristic Indicative of Irma's Overwash Deposit	Presence in Irma's Overwash Deposit				Legend
	Year	Waltz Key	Lower Snipe Key	Blackwater Bay	
Allochthonous nearshore sediments*	2017				Present in 2017
	2019				
Larger mean grain size	2017				Present in 2019
	2019				
Lower organic content	2017				Present in 2017 and statistically distinct (p-value > 0.05)
	2019				
Higher carbonate content	2017				Present in 2019 and statistically distinct (p-value > 0.05)
	2019				
Positive excursion in organic $\delta^{13}\text{C}$	2017				Absent
	2019				
Positive excursion in bulk $\delta^{13}\text{C}$	2017				Not measured
	2019				
Lower C/N	2017				*Not tested for statistical significance
	2019				
Higher abundance of calcareous foraminifera*	2017				*Not tested for statistical significance
	2019				
Higher abundance of marine and brackish diatoms*	2017				*Not tested for statistical significance
	2019				

Fig. 14. Summary table indicating which sedimentological, geochemical, and microfossil characteristics were present within Irma's overwash deposit in November/December 2017 and which remained present until July 2019. Darker shading indicates which characteristics' presence was found to be statistically distinct (p -value < 0.05) compared to mangrove peats. * Indicates which characteristics were only documented for presence/absence and not tested for statistical significance.

mangrove peats through time from Novembers 2017 to July 2019. In doing so, we found:

- Evidence from stratigraphy, grain size analysis, loss-on-ignition, and foraminifera analyses provided the strongest proxy evidence for Irma's overwash event through time. Irma's overwash deposit had a consistently larger mean grain size, lower organic content, and higher carbonate content than underlying mangrove peats in November 2017 and July 2019.
- The carbonate sediment source of Irma's overwash sediments in the Lower Florida Keys and the Ten Thousand Islands provided an additional sedimentological indicator that may not be available in temperate environments but should be utilized in paleo-storm studies in the region.
- Loss-on-ignition and bulk $\delta^{13}\text{C}$ indicators were both successful at distinguishing Irma's carbonate-rich overwash deposit from underlying organic-rich mangrove peats.
- Organic $\delta^{13}\text{C}$ or C/N indicators were not able to discern the marine provenance of Irma's overwash deposit. Therefore, geochemistry did not provide evidence for Irma's overwash event that could not be found by other sedimentological and microfossil analyses.
- Foraminifera were successful in differentiating the calcareous, diverse foraminiferal assemblage of Hurricane Irma's overwash deposit from that of underlying mangrove peats. The presence of the calcareous foraminifera was maintained through time and preserved the evidence of marine inundation via the storm surge into the mangroves.
- Diatoms showed a qualitative change in assemblage between Hurricane Irma's overwash deposit and that of underlying mangrove peats. The relationship between diatoms and local environmental factors was too nuanced to statistically differentiate pre-Irma and Irma sediments within our sampling design.

Repeated sampling of Hurricane Irma's overwash deposit in southern Florida mangroves has shown that the overwash deposits are altered between their time of deposition and when they are incorporated (or excluded) from the geologic record. But regular monitoring of Irma's overwash deposit should continue because the sedimentologic and microfossil characteristics of the deposit are expected to continuously evolve beyond this two-year study period. For example, while foraminifera proved successful in differentiating Hurricane Irma's overwash deposit from underlying mangrove peats over the two-year study period, calcareous foraminifera tests are known to undergo taphonomic alteration and preservation in intertidal sediments through time (Berkeley et al., 2009; Pilarczyk et al., 2014, 2016; Edwards and Wright, 2014).

To maximize the chances of capturing the most complete picture of overwash events available within the geologic record, Irma's overwash deposit has shown that small-scale sampling across sites and within cores is essential. It is possible overwash deposits in southern Florida will be preserved in small clumps of carbonate mud as they were found under mangrove prop roots. A multi-proxy approach based on the local environment, taking into consideration sediment source and local redistribution processes, that includes sedimentological, geochemical, and/or microfossil analyses will yield the highest resolution paleo-storm records. Hurricane Irma's deposit shows, within mangrove ecosystems on carbonate platforms, grain size analysis, loss-on-ignition, and foraminifera are the mostly likely indicators of an overwash deposit to be preserved into the geologic record.

Supplementary data to this article can be found online at <https://doi.org/10.1016/j.margeo.2023.107077>.

Declaration of Competing Interest

The authors declare that they have no known competing financial interests or personal relationships that could have appeared to influence the work reported in this paper.

Data availability

The data supporting this work are openly available in DR-NTU Data at <https://doi.org/10.21979/N9/ZAHOLC>.

Acknowledgements

KMJ thanks Byron Halavik, Melissa Bownik, Scott Adams, Emma Dontis, and Audrey Goeckner for their assistance in collecting sediment samples and survey data. KMJ also thanks Muhammad Hadi Ikhsan for his assistance with graphics. Site access and research permission were provided by B Jessen for the Rookery Bay National Estuarine Research Reserve, M Danaher for the Ten Thousand Islands National Wildlife Refuge (Special Use Permit 41555-2017-R2), and K Watts for the Florida Keys National Wildlife Refuges Complex (Special Use Permit #FFO4RFKD-2015-020). KMJ and REK were supported by NSF awards OCE-1804999, ICER-1663807, ICER-2103754, and DGE-1633557. RPM was supported by a grant from the National Fish & Wildlife Foundation (Grant ID: 2320.17.059025). IH was supported by NSF award EAR 1952740. B.P. Horton was supported by funding from the Ministry of Education Academic Research Fund MOE2019-T3-1-004, the National Research Foundation Singapore, and the Singapore Ministry of Education, under the Research Centres of Excellence initiative. This is a contribution to IGCIP Project 725 "Forecasting Coastal Change". This work is Earth Observatory of Singapore contribution 535. The authors acknowledge PALSEA, a working group of the International Union for Quaternary Sciences (INQUA) and Past Global Changes (PAGES), which in turn received support from the Swiss Academy of Sciences and the Chinese Academy of Sciences.

References

- Admiral, W., 1984. The ecology of estuarine sediment-inhabiting diatoms. *Prog. Phycol. Res.* 3, 269–322.
- Arias, P.A., Bellouin, N., Coppola, E., Jones, R.G., Krinner, G., Marotzke, J., Naik, V., Palmer, M.D., Plattner, G.-K., Rogelj, J., Rojas, M., Sillmann, J., Storelvmo, T., Thorne, P.W., Trevisan, B., Achuta Rao, K., Adhikary, B., Allan, R.P., Armour, K., Bala, G., Barimalala, R., Berger, S., Canadell, J.G., Cassou, C., Cherchi, A., Collins, W., Collins, W.D., Connors, S.L., Corti, S., Cruz, F., Dentener, F.J., Dereczynski, C., Di Luca, A., Diongue Niang, A., Doblas-Reyes, F.J., Dosio, A., Douville, H., Engelbrecht, F., Eyring, V., Fischer, E., Forster, P., Fox-Kemper, B., Fuglested, J.S., Fyfe, J.C., Gillett, N.P., Goldfarb, L., Gorodetskaya, I., Gutierrez, J. M., Hamdi, R., Hawkins, E., Hewitt, H.T., Hope, P., Islam, A.S., Jones, C., Kaufman, D.S., Kopp, R.E., Kosaka, Y., Kossin, J., Krakovska, S., Lee, J.-Y., Li, J., Mauritsen, T., Maycock, T.K., Meinshausen, M., Min, S.-K., Monteiro, P.M.S., Ngoduc, T., Otto, F., Pinto, I., Pirani, A., Raghavan, K., Ranasinghe, R., Ruane, A.C., Ruiz, L., Sallée, J.-B., Samsat, B.H., Sathyendranath, S., Seneviratne, S.I., Sörensson, A.A., Szopa, S., Takayabu, I., Tréguier, A.-M., van den Hurk, B., Vautard, R., von Schuckmann, K., Zaehe, S., Zhang, X., Zickfeld, K., 2021. Technical summary. In: Masson-Delmotte, V., Zhai, P., Pirani, A., Connors, S.L., Péan, C., Berger, S., Caud, N., Chen, Y., Goldfarb, L., Gomis, M.I., Huang, M., Leitzell, K., Lonnoy, E., Matthews, J.B.R., Maycock, T.K., Waterfield, T., Yelekçi, O., Yu, R., Zhou, B. (Eds.), *Climate Change 2021: The Physical Science Basis*. Contribution of Working Group I to the Sixth Assessment Report of the Intergovernmental Panel on Climate Change. Cambridge University Press, Cambridge, United Kingdom and New York, NY, USA, pp. 33–144. <https://doi.org/10.1017/9781009157896.002>.
- Berkeley, A., Perry, C.T., Smithers, S.G., Horton, B.P., Taylor, K.G., 2007. A review of the ecological and taphonomic controls on foraminiferal assemblage development in intertidal environments. *Earth Sci. Rev.* 83 (3), 205–230. <https://doi.org/10.1016/j.earscirev.2007.04.003>.
- Berkeley, A., Perry, C.T., Smithers, S.G., 2009. Taphonomic signatures and patterns of test degradation on tropical, intertidal benthic foraminifera. *Mar. Micropaleontol.* 73, 148–163.
- Blott, S.J., Pye, K., 2001. GRADISTAT: a grain size distribution and statistics package for the analysis of unconsolidated sediments. *Earth Surf. Process. Landf.* 26, 1237–1248.
- Boutton, T.W., 1991. Stable carbon isotope ratios of natural materials: II. Atmospheric, terrestrial, marine, and freshwater environments. In: *Carbon Isotope Techniques*, pp. 173–185.
- Brandon, C.M., Woodruff, J.D., Donnelly, J.P., Sullivan, R.M., 2014. How unique was Hurricane Sandy? Sedimentary reconstructions of extreme flooding from New York Harbor. *Sci. Rep.* 4, 1–9.
- Bregy, J.C., Wallace, D.J., Minzoni, R.T., Cruz, V.J., 2018. 2500-year paleontological record of intense storms for the northern Gulf of Mexico. *Mar. Geol.* 396, 26–42.
- Breithaupt, J.L., Duga, E., Witt, M., Filyaw, R., Friedland, N., Donnelly, M.J., Walters, L. J., Chambers, L.G., 2019. Carbon and nutrient fluxes from seagrass and mangrove wrack are mediated by soil interactions. *Estuar. Coast. Shelf Sci.* 229 (106409), 1–13.
- Breithaupt, J.L., Hurst, N., Steinmuller, H.E., Duga, E., Smoak, J.M., Kominoski, J.S., Chambers, L.G., 2020. Comparing the biogeochemistry of storm surge sediments and pre-storm soils in Coastal Wetlands: Hurricane Irma and the Florida Everglades. *Estuar. Coasts* 43, 1090–1103. Special Issue: Impact of 2017 Hurricanes.
- Campbell, J., Fourqurean, J., 2009. Interspecific variation in the elemental and stable isotope content of seagrasses in South Florida. *Mar. Ecol. Prog. Ser.* 387, 109–123.
- Cangialosi, J.P., Latto, A.S., Berg, R., 2018. Hurricane Irma (Tropical Cyclone Report No. AL112017). National Hurricane Center, pp. 1–111.
- Cariso, A., Kirk, K., Lange, R., Miller, A., 2018. Hurricane Irma (pp. 1–44) [NOAA Water Level and Meteorological Data Report]. National Oceanic and Atmospheric Administration.
- Chappel, A.R., 2018. Soil Accumulation, Accretion, and Organic Carbon Burial Rates in Mangrove Soils of the Lower Florida Keys: A Temporal and Spatial Analysis. University of South Florida St, Petersburg.
- Culver, S.J., Woo, H.J., Oertel, G.F., Buzas, M.A., 1996. Foraminifera of coastal depositional environments, Virginia, U.S.A.; distribution and taphonomy. *PALAIOS* 11 (5), 459–486. <https://doi.org/10.2307/3515213>.
- Das, O., Wang, Y., Donoghue, J., Xu, X., Coor, J., Elsner, J., Xu, Y., 2013. Reconstruction of paleostorms and paleoenvironment using geochemical proxies archived in the sediments of two coastal lakes in Northwest Florida. *Quat. Sci. Rev.* 68, 142–153.
- Dean Jr., W.E., 1974. Determination of carbonate and organic matter in calcareous sediments and sedimentary rocks by loss on ignition: comparison with other methods. *J. Sediment. Petrol.* 44 (1), 242–248.
- Denomme, K.C., Bentley, S.J., Droxler, A.W., 2014. Climatic controls on hurricane patterns: a 1200-y near-annual record from Lighthouse Reef, Belize. *Sci. Rep.* 4 (3876), 1–7.
- Denys, L., 1991. A checklist of the diatoms in the Holocene deposits of the western Belgium coastal plain with a survey of their apparent ecological requirements. In: *Professional Paper of the Geological Survey of Belgium*, p. 41.
- Desianti, N., Enache, M.D., Griffiths, M., Biskup, K., Degen, A., DaSilva, M., Millemann, D., Lippincott, L., Watson, E., Gray, A., Nikitina, D., Potapova, M., 2019. The potential and limitations of diatoms as environmental indicators in Mid-Atlantic Coastal Wetlands. *Estuar. Coasts* 42, 1440–1458.
- Donato, S.V., Reinhardt, E.G., Boyce, J.I., Pilarczyk, J.E., Jupp, B.P., 2009. Particle-size distribution of inferred tsunami deposits in Sur Lagoon, Sultanate of Oman. *Mar. Geol.* 257, 54–64.
- Donnelly, J.P., Webb III, T., 2004. Back-barrier Sedimentary Records of Intense Hurricane Landfalls in the Northeastern United States. In: Murane, R.J., Liu, K. (Eds.), *Hurricanes and Typhoons: Past, Present, and Future*. Columbia University Press, pp. 58–95.
- Donnelly, J.P., Bryant, S.S., Butler, J., Dowling, J., Fan, L., Hausmann, N., Newby, P., Shuman, B., Stern, J., Westover, K., Webb III, T., 2001a. 700 yr sedimentary record of intense hurricane landfalls in southern New England. *GSA Bull.* 113 (6), 714–727.
- Donnelly, J.P., Roll, S., Wengren, M., Butler, J., Lederer, R., Webb III, T., 2001b. Sedimentary evidence of intense hurricane strikes from New Jersey. *Geology* 29 (7), 615–618.
- Donnelly, J.P., Butler, J., Roll, S., Wengren, M., Webb III, T., 2004. A backbarrier overwash record of intense storms from Brigantine, New Jersey. *Mar. Geol.* 210, 107–121.
- Duarte, C., 1990. Seagrass nutrient content. *Mar. Ecol. Prog. Ser.* 67, 201–207.
- Edwards, R., Wright, A., 2014. Foraminifera. In: Shennan, I., Long, A.J., Horton, B.P. (Eds.), *Handbook of Sea-Level Research*, First edition. John Wiley & Sons, Ltd, pp. 191–217.
- Emanuel, K., 2003. Tropical cyclones. *Annu. Rev. Earth Planet. Sci.* 31, 75–104.
- Emery, K.O., Wigley, R.L., Bartlett, A.S., Rubin, M., Barghoorn, E.S., 1967. Freshwater peat on the continental shelf. *Science* 158 (3806), 1301–1307.
- Folk, R.L., Ward, W.C., 1957. Brazos River Bar: a study in the significance of grain size parameters. *J. Sediment. Petrol.* 27 (1), 3–26.
- Fourqurean, J.W., Schrlau, J.E., 2003. Changes in nutrient content and stable isotope ratios of C and N during decomposition of seagrasses and mangrove leaves along a nutrient availability gradient in Florida Bay, FL. *Chem. Ecol.* 19 (5), 373–390.
- Fourqurean, J.W., Zieman, J.C., Powell, G.V.N., 1992. Phosphorus limitation of primary production in Florida Bay: evidence from C:N:P ratios of the dominant seagrass *Thalassia testudinum*. *Limnol. Oceanogr.* 37 (1), 162–171.
- Frankovich, T.A., Gaiser, E.E., Zieman, J.C., Wachnicka, A.H., 2006. Spatial and temporal distributions of epiphytic diatoms growing on *Thalassia testudinum* Banks ex Konig: relationships to water quality. *Hydrobiologia* 569, 259–271.
- Garner, A.J., Mann, M.E., Emanuel, K.A., Kopp, R.E., Lin, N., Alley, R.B., Horton, B.P., DeConto, R.M., Donnelly, J.P., Pollard, D., 2017. Impact of climate change on New York City's coastal flood hazard: increasing flood heights from the preindustrial to 2300 CE. *Proc. Natl. Acad. Sci.* 114 (45), 11861–11866.
- Ginsburg, R.N., 1956. Environmental Relationships of grain size and constituent particles in some South Florida carbonate sediments. *Bull. Am. Assoc. Pet. Geol.* 40 (10), 2384–2427.
- Hawkes, A.D., Horton, B.P., 2012. Sedimentary record of storm deposits from Hurricane Ike, Galveston and San Luis Islands, Texas. *Geomorphology* 171–172, 180–189.
- Hayward, B.W., Grenfell, H.R., Scott, D.B., 1999. Tidal range of marsh foraminifera for determining former sea-level heights in New Zealand. *N. Z. J. Geol. Geophys.* 42 (3), 395–413. <https://doi.org/10.1080/00288306.1999.9514853>.
- He, D., Rivera-Monroy, V.H., Jaffé, R., Zhao, X., 2021. Mangrove leaf species-specific isotopic signatures along a salinity and phosphorus soil fertility gradients in a subtropical estuary. *Estuar. Coast. Shelf Sci.* 248, 106768.
- Hemphill-Haley, E., 1996. Diatoms as an aid in identifying late-Holocene tsunami deposits. *The Holocene* 6 (4), 439–448.

- Hippensteel, S.P., Garcia, W.J., 2014. Micropaleontological evidence of prehistoric Hurricane strikes from Southeastern North Carolina. *J. Coast. Res.* 30 (6), 1157–1172.
- Hippensteel, S.P., Martin, R., E., 1999. Foraminifera as an indicator of overwash deposits, Barrier Island sediment supply, and Barrier Island evolution: Folly Island, South Carolina. *Palaeogeogr. Palaeoclimatol. Palaeoecol.* 149, 115–125.
- Hoffmeister, J.E., Multer, H.G., 1968. Geology and origin of the Florida Keys. *Geol. Soc. Am. Bull.* 79, 1487–1502.
- Hong, I., Pilarczyk, J.E., Horton, B.P., Fritz, H.M., Kosciuch, T.J., Wallace, D.J., Dike, C., Rarai, A., Harrison, M.J., Jockley, F.R., 2018. Sedimentological characteristics of the 2015 Tropical Cyclone Pam overwash sediments from Vanuatu, South Pacific. *Mar. Geol.* 396, 205–214.
- Hong, I., Horton, B.P., Hawkes, A.D., O'Donnell III, R.J., Padgett, J.S., Dura, T., Engelhart, S.E., 2021. Diatoms of the intertidal environments of Willapa Bay, Washington, USA as a sea-level indicator. *Mar. Micropaleontol.* 167, 102033.
- Horton, B.P., Edwards, R.J., 2006. Quantifying Holocene Sea-Level Change using Intertidal Foraminifera: Lessons from the British Isles, 40. Cushman Foundation Special Publication, pp. 1–97.
- Horton, B.P., Sawai, Y., 2010. Diatoms as indicators of former sea levels, earthquakes, tsunamis, and hurricanes. In: Smol, J.P., Stoermer, E.F. (Eds.), *The Diatoms: Applications for the Environmental and Earth Sciences*, Second edition. Cambridge University Press, pp. 357–372.
- Horton, B.P., Rossi, V., Hawkes, A.D., 2009. The sedimentary record of the 2005 hurricane season from the Mississippi and Alabama coastlines. *Quat. Int.* 195, 15–30.
- Javaux, E.J., Scott, D.B., 2003. Illustration of modern benthic foraminifera from Bermuda and remarks on distribution in other subtropical/tropical areas. *Palaeontol. Electron.* 6 (4), 29.
- Kelble, C.R., Johns, E.M., Nuttle, W.K., Lee, T.N., Smith, R.H., Ortner, P.B., 2007. Salinity patterns of Florida Bay. *Estuar. Coast. Shelf Sci.* 71, 318–334.
- Kemp, A.C., Vane, C.H., Horton, B.P., Culver, S.J., 2010. Stable carbon isotopes as potential sea-level indicators in salt marshes, North Carolina, USA. *The Holocene* 20 (4), 623–636.
- Khan, N.S., Vane, C.H., Horton, B.P., 2015a. Stable carbon isotope and C/N geochemistry of coastal wetland sediments as a sea-level indicator. In: Shennan, I., Long, A.J., Horton, B.P. (Eds.), *Handbook of Sea-Level Research*, First edition. John Wiley & Sons, Ltd, pp. 295–311.
- Khan, N.S., Vane, C.H., Horton, B.P., Hiller, C., Riding, J.B., Kendrick, C.P., 2015b. The application of $\delta^{13}\text{C}$, TOC and C/N geochemistry to reconstruct Holocene relative sea levels and paleoenvironments in the Thames Estuary, UK. *J. Quat. Sci.* 30 (5), 417–433.
- Khan, N.S., Vane, C.H., Engelhart, S.E., Kendrick, C., Horton, B.P., 2019. The application of $\delta^{13}\text{C}$, TOC and C/N geochemistry of mangrove sediments to reconstruct Holocene paleoenvironments and relative sea levels, Puerto Rico. *Mar. Geol.* 415 (105963), 1–22.
- Khan, N.S., Ashe, E., Moyer, R.P., Kemp, A.C., Engelhart, S.E., Brain, M.J., Toth, L.T., Chappel, A., Christie, M., Kopp, R.E., Horton, B.P., 2022. Relative Sea-level change in South Florida during the past ~5000 years. *Glob. Planet. Chang.* 216 (103902), 1–19.
- Kiage, L.M., Deocampo, D., McCloskey, T.A., Bianchette, T.A., Hursey, M., 2011. A 1900-year paleohurricane record from Wassaw Island, Georgia, USA. *J. Quat. Sci.* 26 (7), 714–722.
- Kosciuch, T.J., Pilarczyk, J.E., Hong, I., Fritz, H.M., Horton, B.P., Rarai, A., Harrison, M. J., Jockley, F.R., 2018. Foraminifera reveal a shallow nearshore origin for overwash sediments deposited by Tropical Cyclone Pam in Vanuatu (South Pacific). *Mar. Geol.* 396, 171–185.
- Krammer, K., Lange-Berlot, H., 1991a. Bacillariophyceae 3. Teil: Centrales, Fragilariaceae, Eunotiaceae. In: Gerloff, J., Heynig, H., Mollenhauer, D. (Eds.), *Süßwasserflora von Mitteleuropa* (Band 2/3, pp. 576). VEB Gustav Fischer Verlag, Jena.
- Krammer, K., Lange-Berlot, H., 1991b. Bacillariophyceae 4. Teil: Achnantheaceae, Kritische Ergänzungen zu Navicula (Lineolatae) und Gomphonema, Gesamtliteraturverzeichnis Teil 1-4. In: Gerloff, J., Heynig, H., Mollenhauer, D. (Eds.), *Süßwasserflora von Mitteleuropa* (Band 2/4, pp. 437). VEB Gustav Fischer Verlag, Jena.
- Krammer, K., Lange-Bertalot, H., 1986. Bacillariophyceae 1. Teil: Naviculaceae. In: Gerloff, J., Heynig, H., Mollenhauer, D. (Eds.), *Süßwasserflora von Mitteleuropa* (Band 2/1, pp. 876). VEB Gustav Fischer Verlag, Jena.
- Krammer, K., Lange-Bertalot, H., 1988. Bacillariophyceae 2. Teil: Bacillariaceae, Epithemiaceae, Surirellaceae. In: Gerloff, J., Heynig, H., Mollenhauer, D. (Eds.), *Süßwasserflora von Mitteleuropa* (Band 2/2, pp. 610). VEB Gustav Fischer Verlag, Jena.
- Kristensen, E., Bouillon, S., Dittmar, T., Marchand, C., 2008. Organic carbon dynamics in mangrove ecosystems: a review. *Aquat. Bot.* 201–219.
- Kruskal, W.H., Wallis, W.A., 1952. Use of ranks in one-criterion variance analysis. *J. Am. Stat. Assoc.* 47 (260), 583–621.
- Lamb, K., Swart, P.K., 2007. The carbon and nitrogen isotopic values of particulate organic material from the Florida Keys: a temporal and spatial study. *Coral Reefs* 27 (2), 351–362.
- Lamb, A.L., Wilson, G.P., Leng, M.J., 2006. A review of coastal palaeoclimate and relative sea-level reconstructions using $\delta^{13}\text{C}$ and C/N ratios in organic material. *Earth Sci. Rev.* 74, 29–57.
- Lamb, A.L., Vane, C.H., Wilson, G.P., Rees, J.G., Moss-Hayes, V.L., 2007. Assessing $\delta^{13}\text{C}$ and C/N ratios from organic material in archived cores as Holocene Sea level and palaeoenvironmental indicators in the Humber Estuary, UK. *Mar. Geol.* 244, 109–128.
- Lambert, W.J., Aharon, P., Rodriguez, A.B., 2008. Catastrophic hurricane history revealed by organic geochemical proxies in coastal lake sediments: a case study of Lake Shelby, Alabama (USA). *J. Paleolimnol.* 31, 117–131.
- Leatherman, S.P., Williams, A.T., 1977. Lateral textural grading in overwash sediments. *Earth Surf. Process.* 2, 333–341.
- Lin, N., Emanuel, K., Oppenheimer, M., Vanmarcke, E., 2012. Physically based assessment of hurricane surge threat under climate change. *Nat. Clim. Chang.* 2, 462–467.
- Lin, N., Kopp, R.E., Horton, B.P., Donnelly, J.P., 2016. Hurricane Sandy's flood frequency increasing from year 1800 to 2100. *Proc. Natl. Acad. Sci.* 113 (43), 12071–12075.
- Liu, K., 2004. Paleotempestology: Principles, methods, and examples from Gulf Coast Lake Sediments. In: Murane, R.J., Liu, K. (Eds.), *Hurricanes and Typhoons: Past, Present, and Future*. Columbia University Press, pp. 13–57.
- Liu, K., Fearn, M.L., 1993. Lake-sediment record of late Holocene hurricane activities from coastal Alabama. *Geology* 21, 793–796.
- Liu, K., Fearn, M.L., 2000. Reconstruction of prehistoric landfall frequencies of catastrophic Hurricanes in Northwestern Florida from Lake sediment records. *Quat. Res.* 54, 238–245.
- Martin, T., Muller, J., 2021. The geologic record of Hurricane Irma in a Southwest Florida back-barrier lagoon. *Mar. Geol.* 441, 106635.
- McCloskey, T.A., Liu, K., 2012. A sedimentary-based history of hurricane strikes on the southern Caribbean coast of Nicaragua. *Quat. Res.* 78, 454–464.
- McIntire, C.D., 1978. The distribution of estuarine diatoms along environmental gradients: a canonical correlation. *Estuar. Coast. Mar. Sci.* 6 (5), 447–457.
- Meyers, P.A., 1994. Preservation of elemental and isotopic source identification of sedimentary organic matter. *Chem. Geol.* 114, 289–302.
- Milker, Y., Horton, B.P., Nelson, A.R., Engelhart, S.E., Witter, R.C., 2015. Variability of intertidal foraminiferal assemblages in a salt marsh, Oregon, USA. *Mar. Micropaleontol.* 118, 1–16. <https://doi.org/10.1016/j.marmicro.2015.04.004>.
- Mitchell, S., Pilarczyk, J.E., Spiske, M., Jaffe, B., 2021. Nearshore microfossil assemblages in a Caribbean reef environment show variable rates of recovery following Hurricane Irma. *Sedimentology* 1–22.
- Morton, R.A., Gelfenbaum, G., Jaffe, B.E., 2007. Physical criteria for distinguishing sandy tsunami and storm deposits using modern examples. *Sediment. Geol.* 200, 184–207.
- Morvan, J., Debenay, J.-P., Jorissen, F., Redois, F., Bénéteau, E., Delplancke, M., Amato, A.-S., 2006. Patches and life cycle of intertidal foraminifera: implication for environmental and paleoenvironmental interpretation. *Mar. Micropaleontol.* 61 (1), 131–154. <https://doi.org/10.1016/j.marmicro.2006.05.009>.
- Murray, J.W., Alve, E., 2000. Major aspects of foraminiferal variability (standing crop and biomass) on a monthly scale in an intertidal zone. *J. Foraminif. Res.* 30 (3), 177–191. <https://doi.org/10.2113/0300177>.
- NOAA, 2020a. Datums for 8724580, Key West. NOAA Tide and Currents, FL. <https://tidesandcurrents.noaa.gov/datums.html?id=8724580>.
- NOAA, 2020b. Datums for 8725110, Naples, Gulf of Mexico. NOAA Tide and Currents, FL. <https://tidesandcurrents.noaa.gov/datums.html?id=8725110>.
- Oksanen, J., Simpson, G., Blanchet, F., Kindt, R., Legendre, P., Minchin, P., O'Hara, R., Solymos, P., Stevens, M., Szoecs, E., Wagner, H., Barbour, M., Bedward, M., Bolker, B., Borcard, D., Carvalho, G., Chirico, M., De Caceres, M., Durand, S., Evangelista, H., FitzJohn, R., Friendly, M., Furneaux, B., Hannigan, G., Hill, M., Lahti, L., McGlenn, D., Ouellette, M., Ribeiro Cunha, E., Smith, T., Stier, A., Ter Braak, C., Weedon, J., 2022. *vegan: Community Ecology Package*. R package version 2.6–4. <https://CRAN.R-project.org/package=vegan>.
- Parsons, M.L., 1998. Salt marsh sedimentary record of the landfall of Hurricane Andrew on the Louisiana Coast: diatoms and other paleoindicators. *J. Coast. Res.* 14 (3), 939–950.
- Pérez, A., Machado, W., Gutierrez, D., Stokes, D., Sanders, L., Smoak, J.M., Santos, I., Sanders, C.J., 2017. Changes in organic carbon accumulation driven by mangrove expansion and deforestation in a New Zealand estuary. *Estuar. Coast. Shelf Sci.* 192, 108–116.
- Phanthuwongraj, S., Choowong, M., Nanayama, F., Hisada, K., Charusiri, P., Chutakositkanon, V., Pailoplee, S., Chabangbon, A., 2013. Coastal geomorphic conditions and styles of storm surge washover deposits from Southern Thailand. *Geomorphology* 192, 43–58.
- Phleger, F.B., 1965. Living Foraminifera from Coastal Marsh, Southwestern Florida. *Bol. Soc. Geol. Mex.* 28 (1), 45–60.
- Pilarczyk, J.E., Dura, T., Horton, B.P., Engelhart, S.E., Kemp, A.C., Sawai, Y., 2014. Microfossils from coastal environments as indicators of paleo-earthquakes, tsunamis and storms. *Palaeogeogr. Palaeoclimatol. Palaeoecol.* 413, 144–157.
- Pilarczyk, J.E., Horton, B.P., Soria, J.L.A., Switzer, A.D., Siringan, F., Fritz, H.M., Khan, N.S., Ildefonso, S., Doctor, A.A., Garcia, M.L., 2016. Micropaleontology of the 2013 Typhoon Haiyan overwash sediments from the Leyte Gulf, Philippines. *Sediment. Geol.* 339, 104–114.
- R Core Team, 2020. *R: A Language and Environment for Statistical Computing*. R Foundation for Statistical Computing, Vienna, Austria. URL: <https://www.R-project.org/>. URL.
- Rabien, K.A., Culver, S.J., Buzas, M.A., Corbett, D.R., Walsh, J.P., Tichenor, H.R., 2015. The Foraminiferal signature of recent Gulf of Mexico Hurricanes. *J. Foraminif. Res.* 45 (1), 82–105.
- Radabaugh, K.R., Moyer, R.P., Chappel, A.R., Dontis, E.E., Russo, C.E., Joyse, K.M., Bownik, M.W., Goekner, A.H., Khan, N.S., 2020. Mangrove damage, delayed mortality, and early recovery following Hurricane Irma at two landfall sites in Southwest Florida, USA. *Estuar. Coasts* 1–15. Special Issue: Impact of 2017 Hurricanes.
- Reed, A.J., Mann, M.E., Emanuel, K.A., Lin, N., Horton, B.P., Kemp, A.C., Donnelly, J.P., 2015. Increased threat of tropical cyclones and coastal flooding to New York City during the anthropogenic era. *Proc. Natl. Acad. Sci.* 112 (41), 12610–12615.

- Reese, C.A., Strange, T.P., Lynch, W.D., Liu, K., 2008. Geologic evidence of Hurricane Katrina recovered from the Pearl River Marsh, MS/LA. *J. Coast. Res.* 24 (6), 1601–1607.
- Saintilan, N., Khan, N.S., Ashe, E., Kelleway, J.J., Rogers, K., Woodroffe, C.D., Horton, B. P., 2020. Thresholds of mangrove survival under rapid sea level rise. *Science* 368, 1118–1121.
- Sanford, S., 1909. The topography and geology of southern Florida. In: Florida Geological Survey Second Annual Report, pp. 175–231.
- Scalan, R.S., Morgan, T.D., 1970. Isotope ratio mass spectrometer instrumentation and application to organic matter contained in recent sediments. *Int. J. Mass Spectrom.* 4 (4), 267–281.
- Scholl, D.W., 1963. Sedimentation in modern coastal swamps, southwestern Florida. *Bull. Am. Assoc. Pet. Geol.* 47 (8), 1581–1603.
- Schomer, N.S., Drew, R.D., 1982. An Ecological Characterization of the Lower Everglades, Florida bay, and the Florida Keys (82/58.1; FWS/OBS, pp. 1–246). United States Fish and Wildlife Service.
- Schwartz, R.K., 1975. Nature and Genesis of some Storm Washover Deposits (Technical Memorandum TM-61; pp. 1–69). Department of the Army Coastal Engineering Research Center.
- Sicileppi, E., Donnelly, J.P., 2007. Sedimentary evidence of hurricane strikes in western Long Island, New York. *Geochem. Geophys. Geosyst.* 8 (6), 1–25.
- Scott, D.B., Hermelin, J.O.R., 1993. A device for precision splitting of micropaleontological samples in liquid suspension. *J. Paleontol.* 67 (1), 151–154.
- Scott, D.B., Medioli, F.S., 1980. Living vs. total foraminiferal populations: their relative usefulness in paleoecology. *J. Paleontol.* 54 (4), 814–831.
- Scott, D.B., Medioli, F.S., Schafer, C.T., 2007. *Monitoring in Coastal Environments Using Foraminifera and Thecamoebian Indicators*. Cambridge University Press.
- Shapiro, S.S., Wilk, M.B., 1965. An analysis of variance test for normality (complete samples). *Biometrika* 52 (3/4), 591–611.
- Shier, D.E., 1969. Vermetid reefs and coastal development in the Ten Thousand Islands, Southwest Florida. *Geol. Soc. Am. Bull.* 80, 485–508.
- Soria, J.L.A., Switzer, A.D., Pilarczyk, J.E., Siringan, F.P., Khan, N.S., Fritz, H.M., 2017. Typhoon Haiyan overwash sediments from Leyte Gulf coastlines show local variations with hybrid storm and tsunami signatures. *Sediment. Geol.* 358, 121–138.
- Swindles, G.T., Galloway, J.M., Macumber, A.L., Croudace, I.W., Emery, A.R., Wouds, C., Bateman, M.D., Parry, L., Jones, J.M., Selby, K., Rushby, G.T., Baird, A. J., Woodroffe, S.A., Barlow, N.L.M., 2018. Sedimentary records of coastal storm surges: evidence of the 1953 North Sea event. *Mar. Geol.* 403, 262–270.
- Switzer, A.D., Jones, B.G., 2008. Setup, deposition, and sedimentary characteristics of two storm overwash deposits, Abrahams Bosom Beach, Southeastern Australia. *J. Coast. Res.* 24 (1A), 189–200.
- ter Braak, C.J.F., Prentice, I.C., 1988. A theory of gradient analysis. *Adv. Ecol. Res.* 18, 271–317.
- Todd, R., Low, D., 1971. Foraminifera from the Bahama Bank West of Andros Island (Geological Survey Professional Paper No. 683-C; p. 36 pp.). United States Department of the Interior, Geological Survey.
- Troels-Smith, J., 1955. Karakterisering af løse jordarter. Danmarks Geologiske Undersøgelse IV Række 3 (10), 1–73.
- Vane, C.H., Kim, A.W., Moss-Hayes, V., Snape, C.E., Castro Diaz, M., Khan, N.S., Engelhart, S.E., Horton, B.P., 2013. Degradation of mangrove tissues by aboreal termites (*Nasutitermes acajutlae*) and their role in the mangrove C cycle (Puerto Rico): Chemical characterization and organic matter provenance using bulk $\delta^{13}\text{C}$, C/N, alkaline CuO oxidation-GC/MS, and solid-state ^{13}C NMR. *Geochem. Geophys. Geosyst.* 14 (8), 3176–3191.
- Virtanen, P., Gommers, R., Oliphant, T.E., Haberland, M., Reddy, T., Cournapeau, D., Burovski, E., Peterson, P., Weckesser, W., Bright, J., Van Der Walt, S.J., 2020. SciPy 1.0: fundamental algorithms for scientific computing in Python. *Nat. Methods* 17 (3), 261–272.
- Vos, P.C., de Wolf, H., 1993. Diatoms as a tool for reconstructing sedimentary environments in coastal wetlands, methodological aspects. *Hydrobiologia* 269 (1), 285–296.
- Wachnicka, A., Gaiser, E., Collins, L., Frankovich, T., Joseph, B., 2010. Distribution of diatoms and development of diatom-based models for inferring salinity and nutrient concentrations in Florida Bay and Adjacent Coastal Wetlands of South Florida (USA). *Estuar. Coasts* 33, 1080–1098.
- Wang, P., Horwitz, M.H., 2007. Erosional and depositional characteristics of regional overwash deposits caused by multiple hurricanes. *Sedimentology* 54, 545–564.
- Wang, L., Bianchette, T.A., Liu, K., 2019. Diatom evidence of a paleohurricane-induced coastal flooding event in Weeks Bay, Alabama, USA. *J. Coast. Res.* 35 (3), 499–508.
- Wang, Y., Van Beynen, P., Wang, P., Brooks, G., Herbert, G., Tykot, R., 2021. Investigation of sedimentary records of Hurricane Irma in sinkholes, Big Pine Key, Florida. *Prog. Phys. Geogr. Earth Environ.* 1–22.
- Willard, D.A., Bernhardt, C.E., 2011. Impacts of past climate and sea level change on Everglades wetlands: placing a century of anthropogenic change into a late-Holocene context. *Clim. Chang.* 107, 59–80.
- Williams, H.F.L., 2009. Stratigraphy, sedimentology, and microfossil content of Hurricane Rita Storm surge deposits in Southwest Louisiana. *J. Coast. Res.* 25 (4), 1041–1051.
- Williams, H.F.L., 2010. Storm surge deposition by Hurricane Ike on the McFaddin National Wildlife Refuge, Texas: implications for paleotempestology studies. *J. Foraminifer. Res.* 40 (3), 210–219.
- Williams, H.F.L., Flanagan, W.M., 2009. Contribution of Hurricane Rita storm surge deposition to long-term sedimentation in Louisiana coastal woodlands and marshes. *J. Coast. Res.* SI 56, 1671–1675.
- Witkowski, A., Lange-Bertalot, H., Metzeltin, D., 2000. Diatom flora of marine coasts. In: Lange-Bertalot, H. (Ed.), *Iconographia Diatomologica: Annotated diatom micrographs*, vol. 7. Koeltz Scientific Books, p. 925.
- Yang, Z., Myers, E.P., Jeong, I., White, S.A., 2012. *Vdatum for the Coastal Waters from the Florida Shelf to the South Atlantic Bight: Tidal Datums, Marine Grids, and Sea Surface Topography* (NOAA Technical Memorandum NOS CS 27; p. 97). National Oceanic and Atmospheric Administration.
- Zong, Y., Sawai, Y., 2015. Diatoms. In: Shennan, I., Long, A.J., Horton, B.P. (Eds.), *Handbook of Sea-Level Research*, First edition. John Wiley & Sons, Ltd.